International Journal of Geo-Information

MDPI

Article

Spatial Allocation of Elderly Care Resources in High-Density Urban Areas Under the Guidance of Efficiency and Equity

Siyu Zhao [1,2,3], Shaohua Wang [4,5,6,*], Haojian Liang [4], Jingyi Zhou [4], Hao Wang [7], Ning Zhang [8], Chang Liu [4,5] and Hong Gao [1,2,3]

1 Faculty of Geomatics, Lanzhou Jiaotong University, Lanzhou 730070, China; 11240888@stu.lzjtu.edu.cn (S.Z.); gaohong6728@lzjtu.edu.cn (H.G.)
2 National-Local Joint Engineering Research Center of Technologies and Applications for National Geographic State Monitoring, Lanzhou 730070, China
3 Gansu Provincial Engineering Laboratory for National Geographic State Monitoring, Lanzhou 730070, China
4 State Key Laboratory of Remote Sensing and Digital Earth, Aerospace Information Research Institute, Chinese Academy of Sciences, Beijing 100101, China; lianghj@aircas.ac.cn (H.L.); zhoujingyi@aircas.ac.cn (J.Z.); liuchang248@mails.ucas.ac.cn (C.L.)
5 University of Chinese Academy of Sciences, Beijing 100049, China
6 State Key Laboratory of Geographic Information Science and Technology, Institute of Geographic Sciences and Natural Resources Research, Chinese Academy of Sciences, Beijing 100101, China
7 Henan Key Laboratory of Big Data Analysis and Processing, School of Computer and Information Engineering, Henan University, Kaifeng 475004, China; wh_0326@henu.edu.cn
8 China Academy of Urban Planning & Design, Beijing 100044, China; zhangning0496@163.com
* Correspondence: wangshaohua@aircas.ac.cn

Abstract

Rapid urban population aging and increasing land constraints pose significant challenges for improving both service coverage and spatial equity in elderly care facility planning. This study develops an integrated optimization framework that simultaneously addresses accessibility, efficiency, and equity in the spatial allocation of elderly care facilities. First, an improved Gaussian Two-Step Floating Catchment Area (G2SFCA) method is employed to evaluate accessibility patterns across multiple facility types under both walking and driving scenarios. Second, resource allocation equity is quantified using Lorenz curves and spatial Gini coefficients to identify mismatches between elderly care supply and population demand. Building upon these analyses, a fairness-oriented maximum covering location model—termed the Equity Maximum Covering Location Problem (EMCLP)—is formulated and further transformed into a Markov Decision Process. A deep reinforcement learning-based algorithm is subsequently designed to solve the EMCLP under complex spatial constraints. Experiment results demonstrate that the proposed approach achieves improved computational efficiency while maintaining robust solution quality, and effectively enhances service provision in underserved areas through differentiated functional allocation strategies.

Keywords: elderly care facilities; spatial allocation; efficiency–equity trade-off; accessibility; maximum covering location problem; deep reinforcement learning

Check for updates

Academic Editors: Wolfgang Kainz and Wei Huang

Received: 28 April 2026
Revised: 1 July 2026
Accepted: 17 July 2026
Published: 21 August 2026

Copyright: © 2026 by the authors. Published by MDPI on behalf of the International Society for Photogrammetry and Remote Sensing. Licensee MDPI, Basel, Switzerland. This article is an open access article distributed under the terms and conditions of the Creative Commons Attribution (CC BY) license.

1. Introduction

The accelerating pace of population aging has made elderly care a critical issue shaping global socioeconomic systems and public governance [1,2]. As the country with the largest elderly population, China is experiencing rapid and intense aging, accompanied by pronounced regional disparities [3], which places increasing pressure on the adaptability of

urban public service provision systems. Elderly care facilities (ECF), as essential spatial carriers supporting community-based care and ensuring basic livelihood security, have a direct impact on the quality of life and welfare of the elderly population [4]. However, in high-density urban areas characterized by limited land availability and concentrated populations, the mismatch between rapidly evolving demographic structures and insufficient facility capacity has become increasingly evident, leading to significant inequalities in service provision and spatial misallocation [5]. Therefore, achieving precise identification and effective response to elderly care demands in high-density built environments has become a critical measure of a city's capacity to provide public services and the refinement of its governance [6].

The location of elderly care facilities represents a critical topic in urban planning and public policy research, with the primary objective of reconciling the structural tension between the increasing demand for elderly care services and limited public resources. Early studies mainly adopted demand-driven static assessment frameworks, employing methods such as GIS overlay analysis and location entropy to identify the spatial clustering patterns of the elderly population, thereby providing a basis for facility allocation [7,8]. Research focus gradually shifted toward the supply side, emphasizing facility operational efficiency and cost control, and utilizing location-allocation models to minimize overall service costs or travel distances [9]. In recent years, with the continuous enrichment of spatial data and analytical methods, studies have evolved toward integrated supply–demand frameworks, widely applying the two-step floating catchment area (2SFCA) method and its improved variants to quantitatively assess the spatial accessibility of elderly care facilities and to identify patterns of supply–demand imbalance [10,11]. Some studies have further incorporated factors such as environmental quality and land-use compatibility to characterize the comprehensive suitability of facility layouts [12]. However, most of these studies rely on static spatial distribution features and are limited in their ability to capture the dynamic evolution of demand structures and service preferences over time in urban contexts.

Against the backdrop of accelerating population aging and rising demand for public services, improving the efficiency and equity of elderly care resource allocation has become a critical planning issue. Traditional strategies that rely primarily on expanding facility scale are no longer sufficient to address increasingly differentiated and spatially uneven service needs, underscoring the necessity of scientific location optimization to enhance the overall performance of public service systems [13]. In this context, the Maximal Covering Location Problem (MCLP) has been widely adopted in the spatial planning of medical, elderly care, and emergency facilities due to its effectiveness in maximizing service coverage under limited resource constraints [4,14]. By aiming to maximize the population served within predefined coverage thresholds, MCLP provides a fundamental mathematical framework for public facility allocation [15,16]. However, the optimization of elderly care facility locations is not merely a matter of coverage efficiency, but also a complex resource allocation problem that must reconcile spatial efficiency with public service equity [17,18]. Spatial equity, as a core dimension of social sustainability, emphasizes the balanced distribution of service opportunities and the reduction in accessibility disparities among different regions and population groups [19–21]. In high-density urban environments, the relationship between efficiency and equity becomes particularly complex. On the one hand, limited land resources and concentrated populations tend to encourage the spatial concentration of public services in order to maximize coverage efficiency [22]. On the other hand, such concentration may exacerbate accessibility disparities among different neighborhoods and social groups. Consequently, spatial equity should not be viewed merely as an outcome of facility distribution but rather as a dynamic process jointly shaped by facility functions, transportation accessibility, and resource allocation strategies. Understanding these interac-

tions is essential for developing equitable and sustainable elderly care systems in rapidly aging cities [23,24]. Some research has further addressed refined allocation under specific scenarios, including climate-resilient layouts and age-friendly urban development [25,26]. Nevertheless, existing models still tend to prioritize coverage maximization, often overlooking disparities in facility service capacity, the actual accessibility experienced by elderly individuals, and the dynamic evolution of demand over time. To address these limitations, scholars have begun embedding inequality measures—such as the Gini coefficient, Theil index, and Atkinson index—directly into optimization objectives to explicitly quantify trade-offs between efficiency and equity [27,28]. This shift toward multi-objective optimization significantly increases model complexity, transforming elderly care facility location into a high-dimensional, strongly non-linear problem under multiple spatial constraints and dynamic demand conditions [29,30]. Consequently, a critical research gap remains. Traditional location-allocation models prioritize maximizing total covered demand but structurally fail to address spatial disparities, often leaving areas of high demand and low supply severely underserved. While some recent models attempt to incorporate equity constraints using exact solvers or traditional metaheuristics, they face severe computational bottlenecks and lack the adaptability to handle high-dimensional, non-linear spatial trade-offs in megacities. Therefore, a clear methodological advancement is urgently needed to systematically integrate spatial equity at the modeling level and achieve adaptive multi-objective optimization without compromising computational efficiency.

The location of elderly care facilities is typically regarded as a large-scale combinatorial optimization problem, whose complexity grows exponentially with the number of candidate sites and the number of constraints [31]. Traditional exact algorithms often face severe computational efficiency bottlenecks when dealing with high-dimensional constraints, uncertain demand, and equity objectives [32]. To address this, metaheuristic methods such as genetic algorithms, particle swarm optimization, and Tabu search have been widely applied to nonlinear location problems, demonstrating advantages in solution efficiency and robustness [33,34]. In recent years, deep reinforcement learning (DRL) has provided a novel modeling and solution approach for complex facility allocation problems. By representing the location process as a state–action–feedback interactive system, DRL enables the model to continuously adjust allocation strategies under complex constraints [35–37]. Although this approach has achieved relatively mature applications in logistics facility location and transportation resource allocation [38,39], its use in elderly care facility location with integrated spatial equity constraints remains limited. Drawing on recent advances in public safety and resource allocation research [40–42], this study introduces a distinct methodological advancement rather than a mere integration of existing tools. We propose the Equity Maximum Covering Location Problem (EMCLP), a fairness-oriented model solved via a deep reinforcement learning (DRL) framework. Unlike conventional MCLP that treats all covered populations equally, the proposed EMCLP explicitly embeds the spatial Gini coefficient into the objective function to simultaneously optimize service coverage and penalize spatial inequality. Furthermore, instead of relying on static heuristic searches, our DRL approach formulates the facility allocation as a Markov Decision Process. This enables the agent to dynamically learn complex socio-spatial representations and adaptively balance efficiency and equity, overcoming the computational limitations of existing allocation models in high-density urban environments.

This study contributes to equity-oriented facility location optimization by linking accessibility diagnosis, equity assessment, and location-allocation modeling within a coherent methodological process. The accessibility and equity analyses provide an empirical basis for identifying spatial disparities in elderly care services and serve as key inputs for the subsequent optimization model. Building on this foundation, the main methodological

contribution lies in the formulation and solution of an equity-oriented location-allocation problem for elderly care facilities, with particular attention to the balance between coverage efficiency and spatial equity. The main contributions are summarized as follows:

- A population-weighted accessibility and equity assessment framework is established to provide an empirical foundation for subsequent optimization. By integrating the G2SFCA method, Lorenz curves, and the Gini coefficient, the framework systematically identifies spatial disparities in elderly care accessibility across facility types and travel modes.
- An equity-oriented extension of the traditional Maximal Covering Location Problem is developed by incorporating service coverage, population-weighted accessibility inequality, and travel impedance into a unified optimization objective. This formulation enables facility location decisions to balance coverage efficiency with spatial equity, rather than focusing solely on maximizing service coverage.
- A deep reinforcement learning-based solution strategy is proposed to solve the Equity Maximum Covering Location Problem by formulating the sequential facility location process as a Markov Decision Process. Compared with conventional exact and heuristic approaches, the proposed method offers a scalable and adaptive optimization mechanism for addressing high-dimensional spatial constraints and nonlinear efficiency–equity trade-offs.

2. Materials and Methods

2.1. Study Area

Chaoyang District, located in the central urban area of Beijing, is characterized by a large population and diverse functional zones, making it a typical region for studying population structure evolution and aging issues in megacities. The elderly population in the district has been continuously increasing, with high aging and empty-nest phenomena coexisting [43]. As a pioneering area for urban renewal and the development of elderly care service systems, Chaoyang District holds demonstrative significance in promoting the construction of a "15 min elderly care service circle". However, under constrained spatial resources, there remains a notable mismatch between elderly care service supply and population demand: older residential areas are densely populated with concentrated demand, whereas some newly developed communities are inadequately served by elderly care facilities. At the same time, significant differences in pedestrian environments and public transport accessibility across neighborhoods directly affect the equity of elderly access to care services. Against this backdrop, optimizing the spatial allocation of elderly care facilities in high-density urban areas has become a critical issue for alleviating supply–demand conflicts.

2.2. Data Source

This study primarily utilizes points of interest (POI) data for elderly care facilities, gridded elderly population data, and road network data as the foundational datasets for spatial analysis and model construction (Table 1).

Table 1. Data Source.

Data	Data Source
Elderly care facilities POI	https://ditu.amap.com/ (accessed on 16 July 2026)
Elderly population grid	Scientific Data (https://doi.org/10.6084/m9.figshare.27323106.v1)
Road network	OpenStreetMap (https://www.openstreetmap.org (accessed on 16 July 2026))
Building outline	Global 3D Building Footprint Dataset (https://doi.org/10.6084/m9.figshare.28879733)

Multi-source spatial data serve as the analytical basis. The POI data for elderly care facilities are obtained from the Amap platform, including facility categories and spatial locations, and are classified into three types based on service function: daily care, medical and health care, and social and cultural services (Figure 1). Elderly population data are derived from gridded datasets of individuals aged 65 and above, used to characterize the spatial distribution of the elderly population in the study area [44]. Road network data are sourced from OpenStreetMap (OSM) and, after topological correction and attribute filtering, are used to construct a transportation network model for accessibility analysis and spatial optimization. In addition, building spatial data are obtained from the Global Three-Dimensional Building Footprint dataset (3D-GloBFP), with individual buildings as basic units, including building footprints and height information, providing detailed built environment constraints for the study [45].

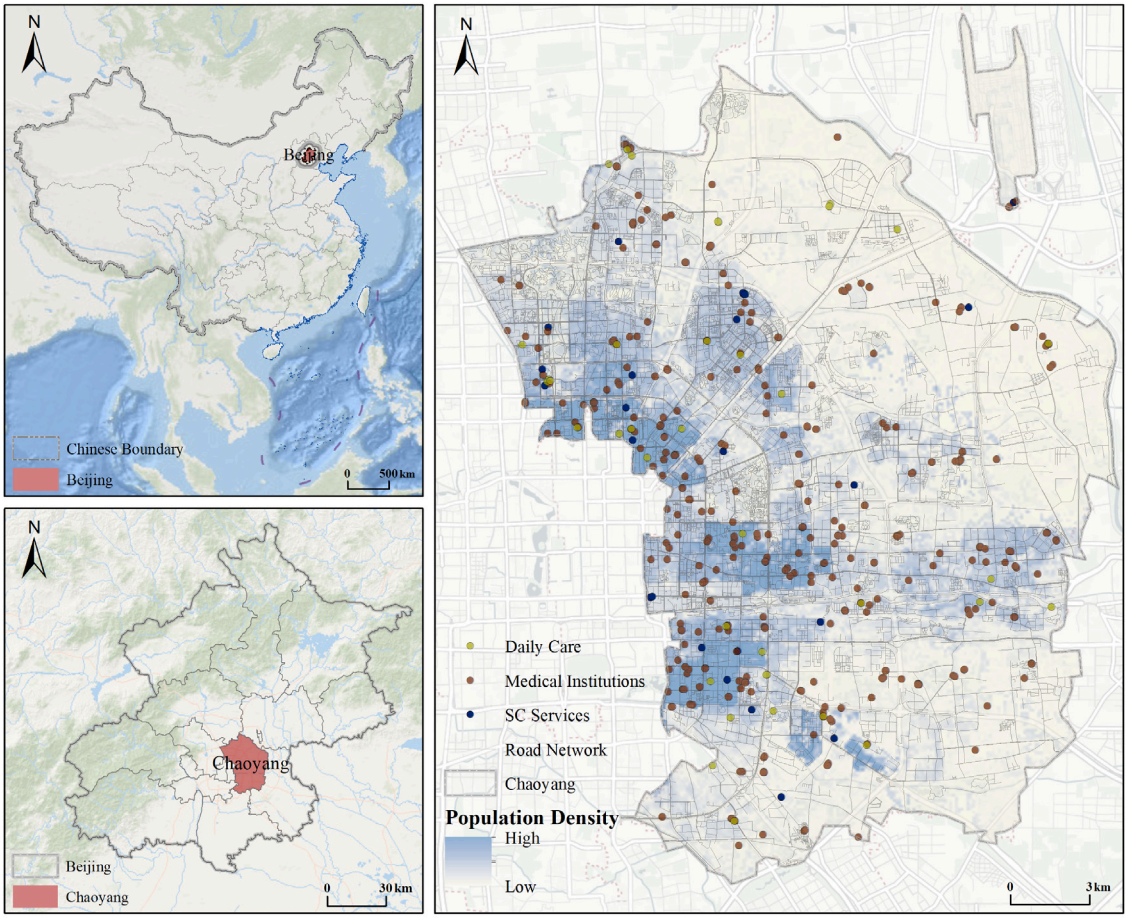


Figure 1. Study Area.

3. Methods

This study focuses on the equitable allocation of elderly care facilities in Chaoyang District under resource constraints, and develops an integrated methodological framework combining accessibility analysis, equity measurement, and deep reinforcement learning-based optimization. The overall research workflow is illustrated in Figure 2. The framework consists of four core stages: data preparation and preprocessing, accessibility assessment, equity evaluation, and equity-oriented facility location optimization, with comparative experiments conducted to systematically evaluate the performance of different optimization strategies. (1) Assessment of spatial distribution and accessibility of different types of elderly care facilities in Chaoyang District: Facilities are categorized into three types, and

accessibility is evaluated under walking and driving scenarios using the Gaussian two-step floating catchment area (G2SFCA) method applied to the road network. (2) Equity analysis of facility allocation: Considering the elderly population and their travel modes, the three types of facilities are quantitatively analyzed for spatial equity, and disparities under different mobility scenarios are compared. (3) Construction of an equity-oriented maximum covering location model (Equity-Oriented Maximal Covering Location Problem, EMCLP): The model integrates spatial equity constraints to guide facility location decisions. (4) Solution of the optimization problem: The EMCLP is solved using a deep reinforcement learning algorithm, with Gurobi Optimizer version 12.0.3 (Gurobi Optimization, LLC, Beaverton, OR, USA) employed as the reference exact solver., and the spatial relationships between the optimized and existing facilities are evaluated using the maximum-minimum distance method.

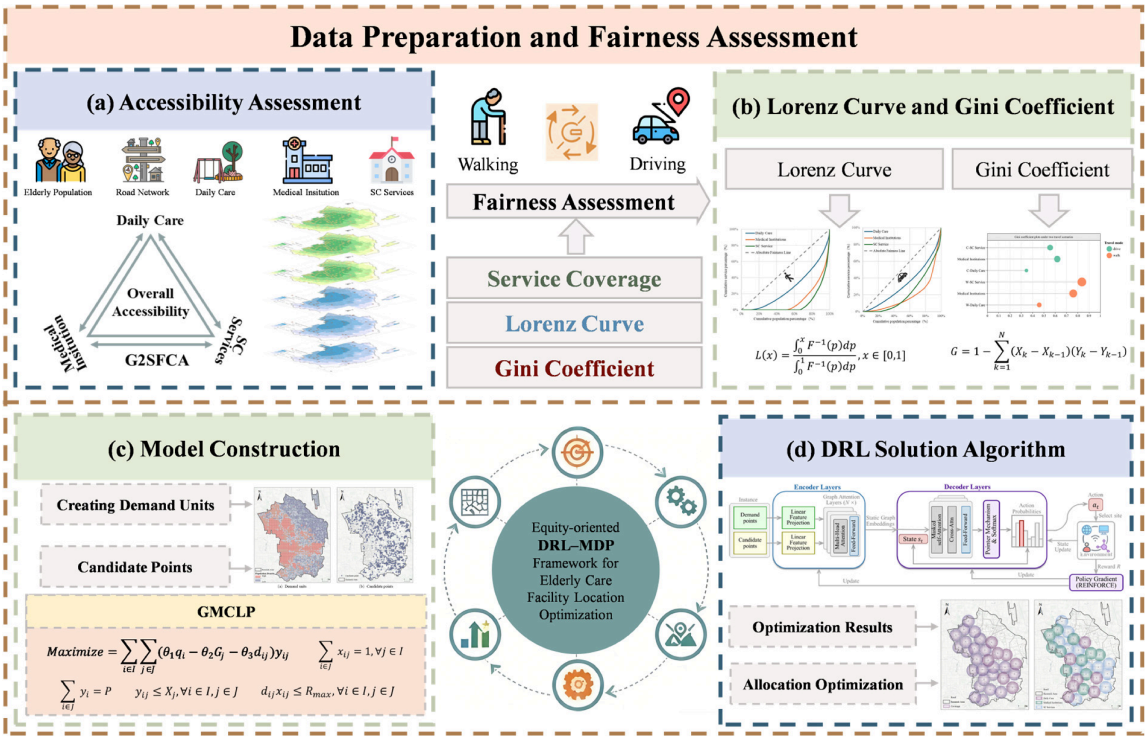


Figure 2. Research framework: (**a**) Accessibility Assessment; (**b**) Lorenz Curve and Gini Coefficient; (**c**) Model Construction; (**d**) DRL Solution Algorithm.

3.1. Spatial Analysis

To scientifically assess the spatial performance of elderly care facilities, the Gaussian two-step floating catchment area (G2SFCA) method is first employed to determine spatial accessibility, followed by the application of the Lorenz curve and Gini coefficient to measure the social equity of resource allocation.

3.1.1. Accessibility Analysis

Accessibility is typically defined as the comprehensive capacity of a demand point to obtain service opportunities within a given spatial structure and transportation conditions. Its general expression can be represented as:

$$A_i = \sum_j S_j f(c_{ij}) \quad (1)$$

Here, A_i represents the accessibility level of demand point i, S_j denotes the service capacity of facility j, c_{ij} is the travel impedance from demand point i to facility j, and

$f(c_{ij})$ is the distance decay function [46]. This indicator captures the interaction among service supply, population demand, and travel cost, and, compared with static measures that consider only facility count or spatial distribution, it more accurately reflects the actual level of public service accessibility.

Given the pronounced functional stratification of elderly care demand and the systematic differences among facility types in service radius and usage frequency, elderly care facilities are classified into three functional categories: daily care services, medical and health care services, and social and cultural services, denoted by $k \in \{1, 2, 3\}$. Meanwhile, accessibility is strongly influenced by variations in elderly mobility. To account for heterogeneous mobility conditions, accessibility is evaluated separately under two travel modes, namely walking and driving, denoted by $m \in \{\text{walk}, \text{drive}\}$.

Under a given travel mode m, the accessibility of demand location i to facilities of functional type k is defined as:

$$A_i^{(k)} = \sum_{j \in k} S_j f(c_{ij}), k \in \{1, 2, 3\} \tag{2}$$

where $\mathcal{F}_k$ denotes the set of facilities belonging to functional category k, S_j represents the service capacity of facility j, c_{ij}^m denotes the travel impedance between demand location i and facility j under travel mode m, and $f(\cdot)$ is the distance-decay function that characterizes the attenuation of service accessibility with increasing travel impedance. This formulation enables stratified measurement of accessibility across facility functional types, allowing the identification of functional inequalities in elderly care service provision.

To further account for mobility differences among elderly populations, the overall accessibility at demand location i under travel mode m is obtained by aggregating accessibility across all facility functional types:

$$A_i^{(m)} = \sum_{k \in \{1,2,3\}} A_{i,m}^{(k)} = \sum_{k \in \{1,2,3\}} \sum_{j \in \mathcal{F}_k} S_j f\left(c_{ij}^m\right), \forall m \in \{walk, drive\} \tag{3}$$

This multi-functional and multi-modal accessibility framework enables comprehensive evaluation of elderly care service accessibility by simultaneously accounting for facility functional heterogeneity and mobility differences, thereby providing a quantitative basis for identifying spatial inequities in elderly care resource allocation.

For impedance calculation, this study conducts network-based accessibility analysis using the actual road network. The road network of the study area, $G(V, E)$, is constructed from OpenStreetMap (OSM) data, and the shortest path distances between demand points and facilities are calculated under different travel scenarios.

$$c_{ij}^m = min \sum_{e \in p} \omega_e^m \tag{4}$$

Here, P_{ij} denotes the set of all feasible paths between demand point i and facility j, and ω_e^m represents the travel cost of road segment e under travel mode m.

To ensure comparability across different mobility scenarios and to improve the reproducibility of the analysis, the spatial travel impedance is explicitly converted into travel time c_{ij}^m based on predefined speed parameters. Aligning with the mobility characteristics of older adults, the average walking speed is set to 2 km/h, while the average driving speed is set to 30 km/h.

Following the standard G2SFCA framework, a Gaussian distance-decay function is employed to model the gradual reduction in service attractiveness. To define the effective facility coverage, a maximum service radius of 2 km is adopted, which reflects the practical service range of community-based elderly care facilities. Based on the respective travel speeds, this 2 km spatial threshold is converted into a time-based catchment threshold (c_0^m)

of 60 min for walking and 4 min for driving. The specific decay function $f(c_{ij}^m)$ is expressed as follows:

$$f\left(c_{ij}^m\right) = \begin{cases} \exp\left(-\frac{1}{2}\left(\frac{c_{ij}^m}{c_0^m}\right)^2\right), c_{ij}^m \le c_0^m \\ 0, \qquad\qquad\qquad c_{ij}^m > c_0^m \end{cases} \tag{5}$$

where c_0^m is the maximum acceptable travel time threshold for mode m. This mathematical formulation guarantees that the distance decay is strictly confined within the 2 km service catchment while accommodating the heterogeneous time impedances of different travel modes.

3.1.2. Spatial Equity Evaluation

To systematically evaluate disparities in the allocation of public service resources across different population groups from a social equity perspective, the Lorenz curve and Gini coefficient are introduced as core evaluation tools [47]. Originally, the Lorenz curve was developed to depict inequalities in income and wealth distribution [48], while the Gini coefficient quantifies the degree of inequality by measuring the area between the Lorenz curve and the line of perfect equality [49]. In recent years, these methods have been widely utilized in studies of public service allocation and spatial accessibility. By identifying spatial mismatches between supply and demand, they offer a rigorous quantitative framework for assessing spatial equity in the distribution of public resources [50,51]. This study evaluates spatial equity from the perspective of population-weighted accessibility. Specifically, accessibility values for each demand grid were first calculated using the G2SFCA model and then weighted according to the corresponding elderly population. Subsequently, Lorenz curves were constructed based on the cumulative proportion of the elderly population and the cumulative proportion of accessibility benefits they received, thereby capturing the equity of elderly care service distribution across the population.

The study area is divided into 5151 grid cells, with the elderly population in each cell i denoted as P_i and the corresponding accessibility to elderly care facilities denoted as A_i. After ranking the accessibility values in ascending order, the cumulative population proportion X_i and the cumulative population-weighted accessibility proportion Y_i can be defined as follows:

$$X_k = \frac{\sum_{i=1}^{k} P_i}{\sum_{i=1}^{N} P_i}, Y_k = \frac{\sum_{i=1}^{k} E_i}{\sum_{i=1}^{N} E_i} \tag{6}$$

Here, Y_i is population-weighted, which accurately reflects the influence of population size on the equity assessment. The Lorenz curve, plotted from (X_i, Y_i), provides an intuitive representation of the spatial and population-based distribution inequalities of elderly care resources.

$$L(x) = \frac{\int_0^x F^{-1}(p)dp}{\int_0^1 F^{-1}(p)dp}, x \in [0,1] \tag{7}$$

The Gini coefficient G is used to quantitatively characterize the degree of inequality in resource allocation, and its discrete form can be expressed as follows:

$$G = 1 - \sum_{k=1}^{N} (X_k - X_{k-1})(Y_k - Y_{k-1}) \tag{8}$$

The Gini coefficient ranges from 0 to 1, where (G = 0) indicates perfect equity and (G = 1) represents extreme inequality. In this study, the Gini coefficient is not calculated based on spatial units themselves, but rather on the population-weighted distribution of accessibility among elderly residents. Specifically, the Lorenz curve is constructed using the cumulative proportion of the elderly population on the horizontal axis and the

cumulative proportion of accessibility benefits received by that population on the vertical axis. Therefore, the resulting Gini coefficient reflects inequality in accessibility opportunities experienced by elderly population groups rather than simple differences among grid cells.

Accordingly, the equity concept adopted in this study is more precisely defined as "population-weighted accessibility equity", which evaluates the extent to which elderly residents have equitable access to elderly care services. While closely related to the broader concept of spatial equity, it primarily captures the distributional fairness of accessibility and does not explicitly account for other dimensions of equity, such as socioeconomic vulnerability, health conditions, disability status, or service affordability.

Elderly care services exhibit substantial heterogeneity in both functional characteristics and travel behavior, making it difficult for a single aggregate indicator to fully represent their equity performance. To capture these differences, elderly care facilities are classified into three categories: daily care services, medical and health care services, and social and cultural services. Accessibility is calculated separately for each facility category and travel mode, denoted as $A_i^{(k,m)}$, where k represents the facility type and m denotes the travel scenario.

$$Y_i^{(k,m)} = \frac{\sum_{j=1}^{i} A_j^{(k,m)} P_j}{\sum_{j=1}^{N} A_j^{(k,m)} P_j} \tag{9}$$

$$G = 1 - \sum_{k=1}^{N} (X_k - X_{k-1})(Y_k - Y_{k-1}) \tag{10}$$

where G_j denotes the accessibility-based Gini coefficient of facility type j (Daily Care, Medical Institutions, or SC Service), which is used to quantify the existing level of spatial inequality for each facility category.

3.2. Model Building

This study develops an equity-oriented maximal covering location model (EMCLP), which incorporates allocation equity constraints to achieve balanced optimization of resource distribution.

$$Maximize \sum_{i \in I} \sum_{j \in J} (\theta_1 q_i - \theta_2 G_j - \theta_3 d_{ij}) y_{ij} \tag{11}$$

$$\sum_{i \in J} x_{ij} = 1, \forall j \in I \tag{12}$$

$$\sum_{i \in J} y_i = P \tag{13}$$

$$y_{ij} \leq X_j, \forall i \in I, j \in J \tag{14}$$

$$d_{ij} x_{ij} \leq R_{max}, \forall i \in J, j \in I \tag{15}$$

The three weighting parameters in the EMCLP objective function reflect different planning priorities: θ_1 for elderly demand coverage, θ_2 for the Gini-related inequality penalty, and θ_3 for the travel-distance penalty. The baseline setting ($\theta_1, \theta_2, \theta_3$ = 0.7, 0.2, 0.1) prioritizes demand coverage while accounting for equity and distance efficiency. All objective components (q_i, G_j, and d_{ij}) were normalized before aggregation to ensure comparability. To assess the robustness of this baseline configuration, a sensitivity analysis was conducted by varying the three weights while keeping all other model settings unchanged. The parameters and their meanings are shown in Table 2.

Table 2. Parameters and meanings.

Parameter	Meaning
I	Demand points
J	Candidate locations
i	The i-th requirement point, $i \in I$
j	Index of candidate facility locations, $j \in J$
q_i	Demand intensity at point i
d_{ij}	The travel time or distance from demand point i to facility j.
R_{max}	Maximum service radius of the facility
y_{ij}	If demand point i is covered by facility j, then the value is 1; otherwise, it is 0.
P	Total number of facilities
G_j	Scheme-level population-weighted accessibility Gini coefficient
θ_1	Service utility coefficient
θ_2	Inequality aversion parameter
θ_3	Space impedance factor
X_j	Binary decision variable indicating whether candidate facility location j is selected (1 = yes, 0 = no)

It should be noted that the Gini coefficient in the EMCLP objective function is not treated as an intrinsic attribute of an individual candidate site. Instead, it is used as a scheme-level equity penalty calculated from the population-weighted accessibility distribution generated by a given facility-location solution. In the sequential optimization process, the contribution of each candidate site to the equity objective is reflected by its marginal impact on the overall accessibility inequality after it is selected.

3.3. Algorithm Design

To optimize the spatial allocation of elderly care facilities under multi-constraint and nonlinear complex environments, a deep reinforcement learning (DRL) approach is introduced, formalizing the facility location problem as a Markov Decision Process (MDP). This approach enables the learning of optimal location strategies through continuous interaction within a high-dimensional state space, effectively overcoming the efficiency and stability limitations faced by traditional heuristic algorithms under complex spatial structures and equity constraints. Figure 3 illustrates the framework of the DRL-based elderly care facility location algorithm.

The algorithm formulates the elderly care facility location optimization problem as an MDP, in which an agent interacts continuously with the spatial environment to seek the optimal solution. The framework consists of five components, which are defined as follows:

State S_t: The state S_t represents the configuration of elderly care facilities x_i at each time step, the coverage status of demand points y_i, the spatial locations of demand points h, and the spatial locations of facility points v.

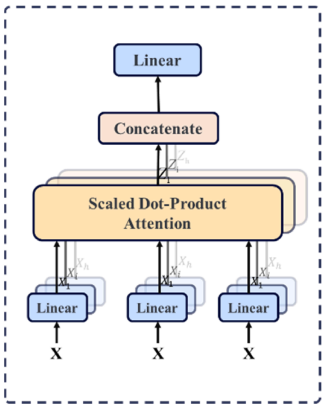
$$S_t = (\{y_i\}_{i \in I}, \{x_i\}_{j \in J}, h, v) \tag{16}$$

Action space a_t: The action a_t represents, at decision step t, the selection of an optimal grid cell (i, j) from the candidate set C to place a specific type of elderly care facility. It is formally defined as follows:

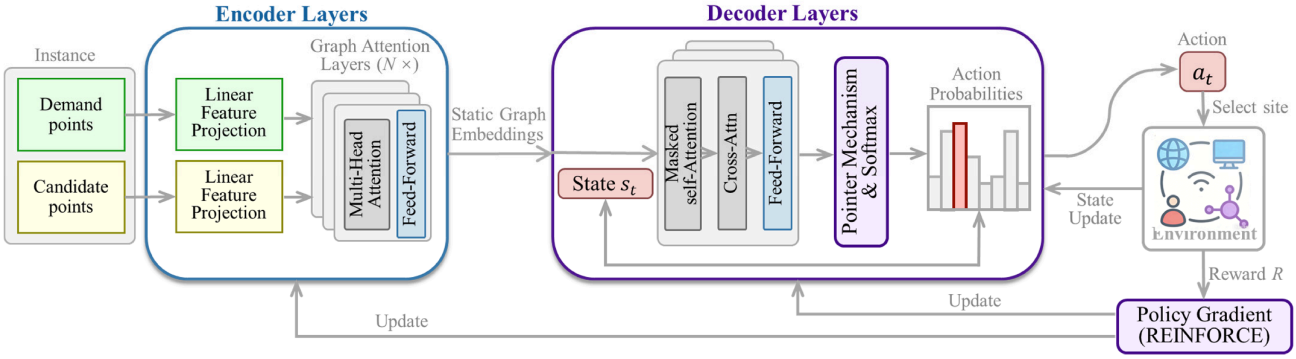
$$a_t = j_t, j_t \in J \tag{17}$$

State Transition: A state transition represents the progression from the current state S_t to the next state as a result of the model taking action a_t. When the agent selects a facility

location, the environment updates the service accessibility and the scheme-level spatial equity indicator based on that action.



(**a**) Multi-head attention mechanism



(**b**) The network structure of deep reinforcement learning

Figure 3. The architecture of the deep reinforcement learning model for elderly care facility location optimization: (**a**) Multi-head attention mechanism. (**b**) The network structure of deep reinforcement learning.

These changes are then fed back to the system, driving the environment to evolve into the next decision stage.

Reward Function R: The reward function is the core criterion for evaluating decision quality. The system calculates the reward based on changes in elderly care service efficiency and the overall scheme-level spatial equity before and after each facility location decision, thereby guiding the model to adjust its parameters toward a global optimum.

$$r_t = \sum_{i \in I} \left(\theta_1 q_i - \theta_2 G_{jt} - \theta_3 d_{ijt}\right) \Delta y_{ij} \tag{18}$$

Discount Factor γ: The discount factor γ is set to 1, reflecting the principle that the optimization of elderly care facility layout should prioritize the overall social welfare of the final solution. Unlike approaches that focus on the immediate reward of individual facility locations, this setting ensures that the model concentrates on the long-term cumulative service effectiveness and the global equity of spatial allocation after all facilities are established. The overall policy $p(\pi|s)$ can be expressed as:

$$P_\theta(\pi|s) = \prod_{t=1}^{p} P_\theta(\pi_t|s_t, \pi_{1t-1}), p \leq n \tag{19}$$

Encoder-Spatial Feature Representation: The algorithm adopts an encoder–decoder architecture to efficiently represent complex spatial information and generate facility lo-

cation strategies. The encoder, positioned at the front end of the model, is responsible for jointly modeling multi-source spatial data and embedding them into a unified latent representation space.

During the encoding phase, the original features of demand points and candidate sites (denoted as f_i) are first projected into a unified high-dimensional vector space through linear feature mapping, yielding the initial embeddings $h_i^{(0)} = W_x f_i$, where W_X is a learnable weight matrix. This step eliminates scale discrepancies among heterogeneous feature dimensions.

Subsequently, a multi-layer Graph Attention Network (GAT) is employed to model the topological relationships among spatial points. As illustrated in Figure 3a, we utilize the Scaled Dot-Product Attention mechanism. For each node i, its embedding is linearly projected to generate queries q_i, keys k_i, and values v_i. By adaptively assigning attention weights, the model effectively captures the spatial association intensity between densely populated areas and surrounding candidate facilities. The attention coefficient α_{ij} between node i and its neighbor j is calculated as:

$$\alpha_{ij} = \text{softmax}\left(\frac{q_i k_j^T}{\sqrt{d_k}}\right) = \frac{\exp\left(\frac{q_i k_j^T}{\sqrt{d_k}}\right)}{\sum_{n\in(i)} \exp\left(\frac{q_i k_n^T}{\sqrt{d_k}}\right)} \tag{20}$$

where d_k is the dimension of the key vectors, and $\mathcal{N}(i)$ denotes the neighborhood of node i. The node representations are then updated by aggregating the weighted values from their neighbors:

$$h_i^{(l)} = \sum_{j\in(i)} \alpha_{ij} v_j \tag{21}$$

After multiple rounds of attention aggregation (l layers), the encoder outputs a set of static graph embedding vectors, which compress the global geographic information of the study area and provide a stable environmental representation for subsequent decisions.

Decoder: Sequential Action Generation

Building on this, the decoder is responsible for generating specific facility location decisions, and its architecture is designed to emulate stepwise reasoning and sequential decision-making processes. The decoding state at step t is denoted as c_t, which encodes the context of previously selected facility locations.

During the decoding phase, a masked self-attention mechanism is introduced to dynamically block already selected sites and candidate locations that violate planning constraints, ensuring that each decision is made only within a legal candidate set. Simultaneously, the decoder employs a cross-attention mechanism to align the current decision state c_t with the global environmental embeddings h_j produced by the encoder.

During the decision output phase, the decoder utilizes a Pointer Mechanism to compute attention scores $u_{t,j}$ for all candidate sites $j \in J$:

$$u_{t,j} = v^T \tanh(W_1 c_t + W_2 h_j) \tag{22}$$

where v, W_1, W_2 are learnable parameters. To enforce the aforementioned spatial and capacity constraints, a dynamic mask $M_{t,j}$ is applied, where $M_{t,j} = -\infty$ if site j is already selected or deemed invalid, and 0 otherwise. Finally, these scores are passed through a Softmax function to form the action probability distribution for step t:

$$\pi_\Theta(a_t = j|s_t) = \text{softmax}(u_{t,j} + M_{t,j}) = \frac{\exp(u_{t,j} + M_{t,j})}{\sum_{k\in J} \exp(u_{t,k} + M_{t,k})} \tag{23}$$

The site with the highest probability is then selected (or sampled during training) as the optimal construction location a_t for the current step. This sequence of conditional probabilities forms the basis for the subsequent policy gradient optimization.

Training of the DRL Agent: To optimize the parameters of the encoder and decoder networks (collectively denoted as Θ), we employ the REINFORCE algorithm, a prominent Policy Gradient method. As illustrated in the rightmost section of Figure 3b, the DRL agent interacts with the spatial environment by sequentially selecting facility sites a_t based on the action probabilities generated by the Pointer Mechanism. The ultimate objective of the training process is to learn the optimal network parameters Θ that maximize the expected cumulative reward J(Θ) over a complete episode (i.e., the selection of all P facilities):

$$J(\Theta) = \mathbb{E}_{\pi_\Theta}\left[\sum_{t=1}^{P} r_t\right] = \mathbb{E}_{\pi_\Theta}[R] \tag{24}$$

where π_Θ represents the stochastic policy parameterized by the deep neural networks, and Ris the total cumulative reward evaluated at the end of the episode, which incorporates both service coverage efficiency and solution-level spatial equity measured by the population-weighted accessibility Gini coefficient.

A direct implementation of the standard REINFORCE algorithm often suffers from high variance during training, primarily because the absolute value of the reward R in spatial coverage problems is strictly positive. To stabilize the learning process and accelerate convergence, we introduce a baseline b into the policy gradient formulation. By subtracting this baseline, the model evaluates the advantage of the selected actions rather than their absolute performance. The gradient of the objective function is mathematically derived as follows:

$$\nabla_\Theta J(\Theta) \approx \frac{1}{B}\sum_{i=1}^{B}\sum_{t=1}^{P} \nabla_\Theta \log \pi_\Theta(a_{i,t}|s_{i,t})(R_i - b) \tag{25}$$

where B is the batch size, R_i is the total reward for the i-th instance in the batch, and b is the baseline value, which is updated using the exponential moving average (EMA) of historical rewards. The term $(R_i - b)$ evaluates whether the current location strategy performs better or worse than the historical average.

During the training phase, the gradients are backpropagated through the network architecture. The parameters of both the Encoder and Decoder layers are iteratively updated via gradient ascent using the Adam optimizer. This process corresponds exactly to the "Policy Gradient (REINFORCE)" module and the "Update" pathways depicted in Figure 3b. The detailed training procedure of the proposed DRL model is summarized in Algorithm 1.

Algorithm 1 Deep Reinforcement Learning Training Procedure for EMCLP

Input: Set of demand points I, Set of candidate locations J, Number of facilities to locate P
Hyperparameters: Batch size B, Learning rate η, Baseline decay rate α, Max training epochs E
Output: Optimized network parameters Θ
Initialize network parameters Θ with random weights
Initialize baseline $b = 0$
for epoch = 1 to E do
Initialize batch gradients $d\Theta = 0$
for $i = 1$ **to** B **do**
Reset environment and observe initial state $s_{i,1}$

Algorithm 1 *Cont.*

Generate static graph embeddings via the Encoder (GAT)
for $t = 1$ **to** P **do**
Compute action probabilities $\pi_{\Theta}(a_t|s_{i,t})$ via the Decoder
Sample an action $a_{i,t} \in J$ based on π_{Θ}
Update environment state $s_{i,t+1}$ and apply spatial mask to $a_{i,t}$
end for
Evaluate the final spatial allocation to compute total reward R_i (Equation (17))
end for
//Update baseline using Exponential Moving Average
$b \leftarrow \alpha b + (1-\alpha)\frac{1}{B}\sum_{i=1}^{B} R_i$
//Compute Policy Gradient with baseline
$\nabla_{\Theta} J(\Theta) = \frac{1}{B}\sum_{i=1}^{B}\sum_{t=1}^{P} \nabla_{\Theta} log\pi_{\Theta}(a_{i,t}|s_{i,t})(R_i - b)$
//Update network parameters using Adam optimizer
$\Theta \leftarrow \Theta + \eta \nabla_{\Theta} J(\Theta)$
end for
return Θ

4. Results

4.1. Spatial Distribution Characteristics and Equity Assessment of Elderly Care Service Resources

First, a baseline assessment is conducted on the spatial allocation of elderly care service resources in Chaoyang District, Beijing. By systematically analyzing accessibility differences under various travel modes and combining the Lorenz curve with the Gini coefficient to identify structural features of supply–demand imbalance, the study provides empirical evidence to inform subsequent facility location optimization.

4.1.1. Accessibility of Elderly Care Services Under Multiple Travel Modes

In this section, the spatial accessibility differentiation of elderly care facilities in Chaoyang District is systematically analyzed under two travel modes—walking and driving—based on network travel costs. The accessibility of three types of elderly care facilities under these two travel scenarios is evaluated, as shown in Figure 4, reflecting the differences among populations with varying mobility capabilities.

Under the walking scenario, the overall accessibility of elderly care service resources is relatively low, with the accessibility distributions of all three facility types predominantly at lower levels. For daily care facilities, 41.90% of the population falls within the lowest accessibility category, indicating that most older adults have limited convenience in accessing basic daily care services on foot. The accessibility of medical institutions is even more concentrated at lower levels, with the cumulative proportion of the population in the lowest and low accessibility categories reaching 74.56%, highlighting a significant deficiency in service coverage for medical resources under walking conditions. Cultural, recreational, and social service facilities exhibit the lowest walking accessibility, with over 75% of the population in low-accessibility categories, reflecting the relatively limited service provision capacity of this facility type under the current travel conditions.

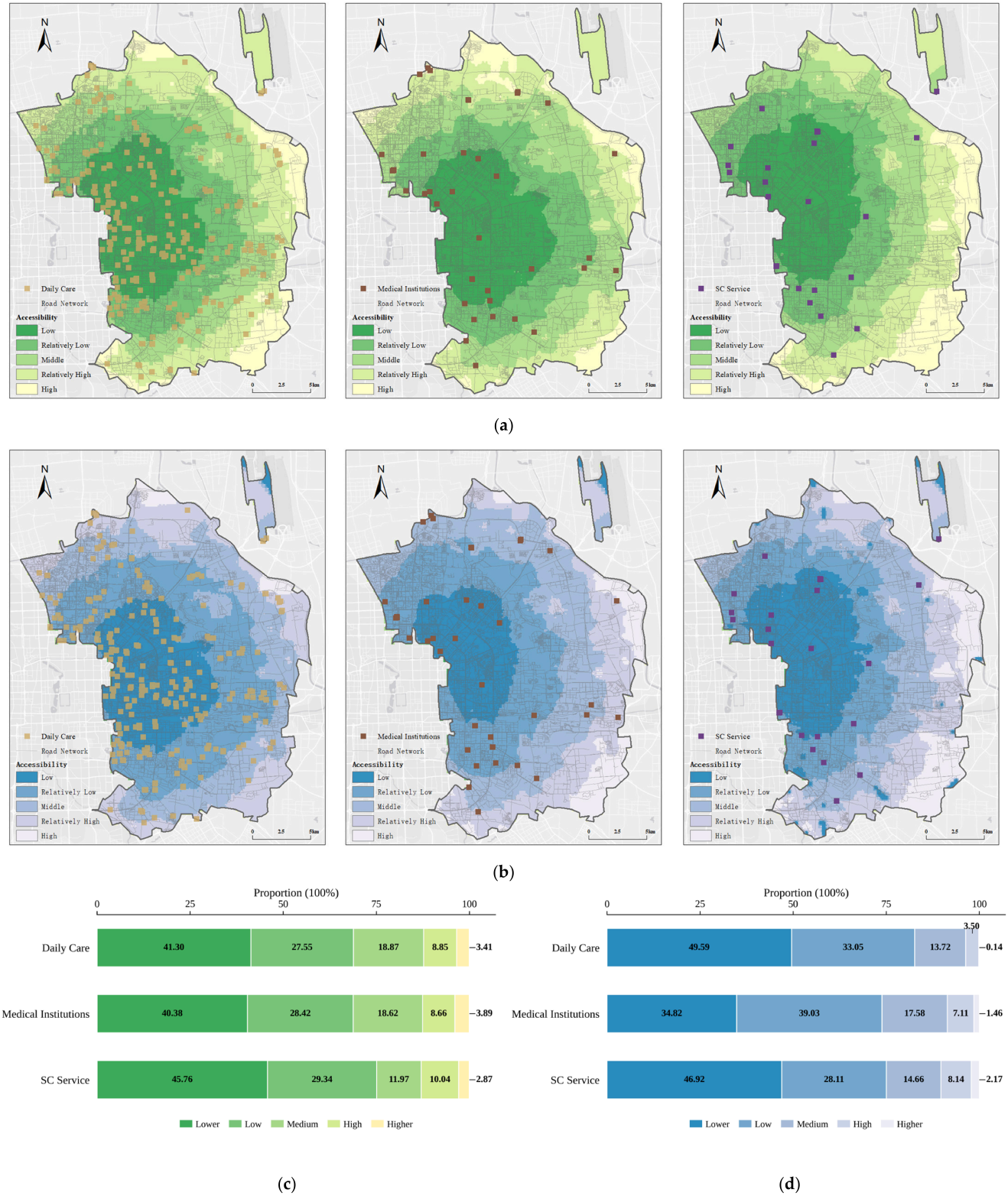


Figure 4. Comparative analysis of spatial accessibility and structural characteristics of elderly care facilities based on multi-travel modes: (**a**) Accessibility analysis of three types of facilities in walking mode. (**b**) Accessibility analysis of three types of facilities under the driving mode. (**c**) Coverage rate of the elderly population within walking distance. (**d**) The coverage rate of the elderly population under driving conditions.

Under the driving scenario, the overall accessibility of elderly care service resources improves markedly, with a substantial increase in the proportion of the population at

medium and high accessibility levels. For daily care facilities, the proportion of the population in the lowest accessibility category decreases to 0.50%, while the cumulative proportion at medium and higher accessibility levels reaches 90.60%, indicating that improved transportation conditions effectively expand the service coverage of this facility type. Medical institutions also show significant improvement under driving conditions, with the proportion of the population at medium and higher accessibility levels increasing to 66.15%, demonstrating the strong spatial extensibility of medical resources supported by the transportation network. In contrast, the accessibility of cultural, recreational, and social service facilities improves only moderately, with 46.92% of the population remaining in the lowest accessibility category, suggesting that the insufficient spatial provision of this facility type has a certain structural characteristic.

Overall, the spatial accessibility of elderly care facilities in Chaoyang District exhibits pronounced differences across travel modes. The accessibility patterns under the walking scenario reveal insufficient local coverage of elderly care service resources, whereas the driving scenario alleviates this limitation to some extent; however, disparities in accessibility among different facility types persist. These findings provide an important empirical foundation for subsequent assessments of the spatial equity of elderly care service resources and for the optimization of facility layout.

4.1.2. Quantitative Identification and Analysis of Supply and Demand Imbalance

The distributional patterns revealed by the Lorenz curves provide a basis for analyzing the equity of elderly care service resource allocation. As shown in Figure 5, under both walking and driving scenarios, the accessibility Lorenz curves for the three types of elderly care facilities deviate markedly from the line of absolute equality, exhibiting varying degrees of curvature. This indicates that accessibility to elderly care facilities is unevenly distributed among the elderly population, characterized by a small proportion of residents enjoying relatively high service levels while the majority experience comparatively low accessibility. A further comparison of the two travel scenarios shows that the degree of deviation from the equality line is generally greater under the walking scenario than under the driving scenario, suggesting that supply–demand imbalances in elderly care services become more pronounced when travel conditions are constrained.

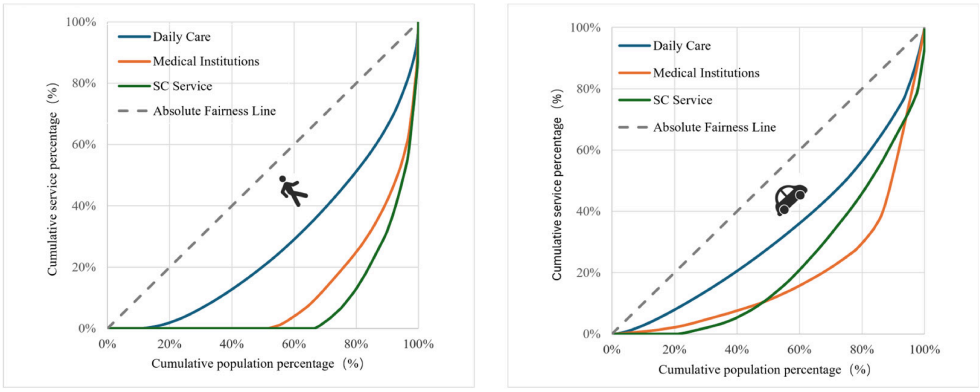


Figure 5. Lorenz curves for two travel scenarios: (**a**) Lorenz curves in walking state. (**b**) Lorenz curves under drive motion conditions.

To further quantify the degree of inequality across facility types and travel modes, the Gini coefficient is introduced as a quantitative measure. The results are presented in Figure 6. Under the walking scenario, the spatial Gini coefficients of the three types of elderly care facilities are generally high, with notable differences among facility types.

Cultural, recreational, and social service facilities exhibit the highest level of inequality, with a Gini coefficient of 0.837, indicating a highly concentrated accessibility distribution. Medical care facilities also show substantial inequality, with a Gini coefficient of 0.760. In contrast, daily living care facilities have a relatively lower Gini coefficient of 0.459, although they still fall within the range of inequitable distribution. These findings further suggest that, compared with basic daily care services, higher-level elderly care services are more prone to spatial concentration.

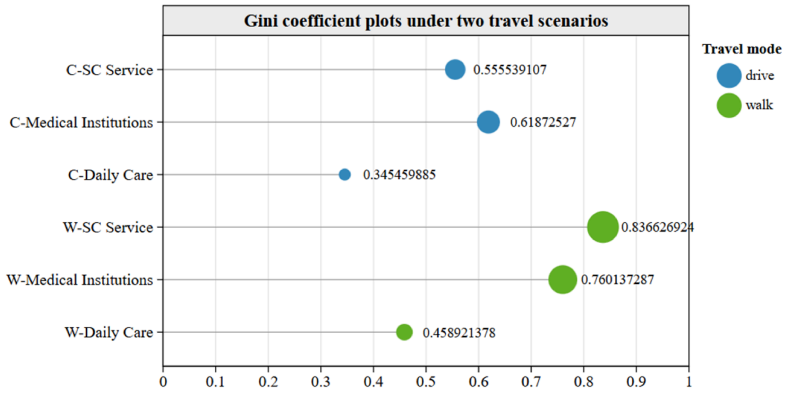


Figure 6. Gini coefficient plots under two travel modes.

When the travel mode shifts from walking to driving, the spatial Gini coefficients for all facility types decrease overall, yet inequality is not fully eliminated. The Gini coefficients for medical care facilities and cultural, recreational, and social service facilities decline to 0.619 and 0.556, respectively, remaining at relatively high levels, whereas daily living care facilities show the most pronounced improvement in equity, with the Gini coefficient dropping to 0.345. This comparison indicates that improved transportation conditions can partially mitigate disparities in accessibility to elderly care facilities. Taken together, the combined analysis of the Lorenz curves and spatial Gini coefficients reveals persistent supply–demand mismatches in the configuration of elderly care facilities in Chaoyang District, with substantial variations in inequality across different facility types. These findings underscore the importance of incorporating equity constraints into elderly care facility layout optimization and provide a clear problem formulation and empirical data foundation for the subsequent development of a deep reinforcement learning-based facility location optimization approach.

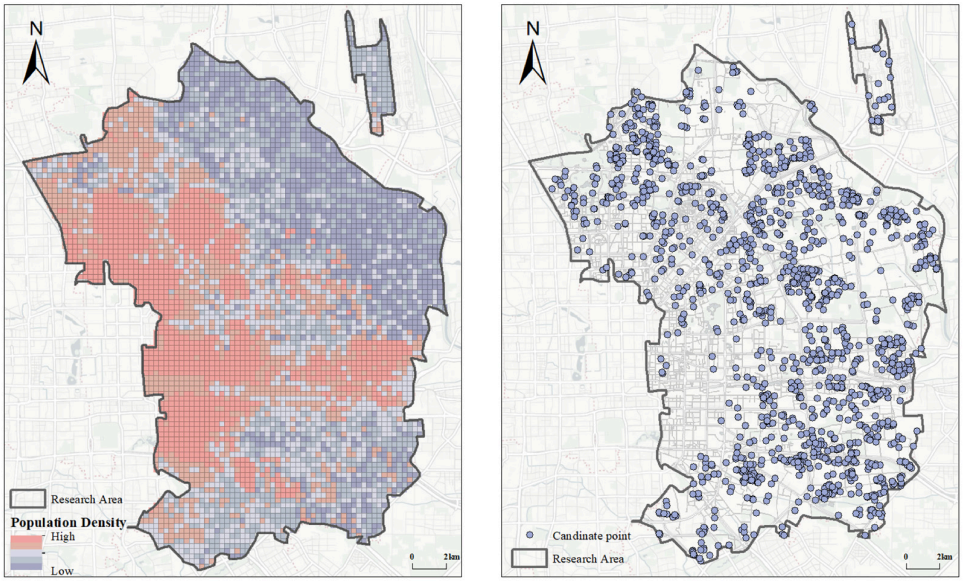
4.2. Experimental Evaluation and Optimization Results

4.2.1. Experimental Preparation

A 300 m grid was adopted as the basic analytical unit, with the geometric centroid of each grid cell defined as a demand point, resulting in a total of 5151 demand points. Based on gridded elderly population density data, each demand point was assigned a corresponding elderly population demand intensity, thereby representing the potential level of elderly care service demand across different spatial units.

Candidate facility locations were extracted using the geometric centroids of buildings and further refined through a multi-stage filtering process incorporating building attribute information. Specifically, buildings constructed in earlier periods and associated with high renovation difficulty were first excluded. Subsequently, building types unsuitable for elderly care facilities—such as industrial buildings and large transportation-related land uses—were removed. In addition, buildings with insufficient floor area and thus incapable of meeting functional requirements were eliminated. Following this screening

procedure, a total of 1500 candidate elderly care facility locations were identified. The spatial distribution characteristics of these candidate sites are illustrated in Figure 7.



(**a**) (**b**)

Figure 7. Spatial distribution of analytical units and candidate facility locations: (**a**) Demand units. (**b**) Candidate facility locations.

4.2.2. Experimental Settings and Evaluation Metrics

The proposed DRL algorithm was implemented using the PyTorch framework. All experiments were conducted on a workstation equipped with an Intel Xeon Gold 6530 CPU and an NVIDIA GeForce RTX 4090 GPU with 24 GB of memory. The software environment consisted of Python 3.9 and PyTorch 1.13.1, and Conda 22.9.0 was used for environment management to ensure reproducibility. To simulate practical elderly care facility location scenarios, 128,000 training instances were generated for each scenario configuration, with an additional 2000 validation instances and 2000 test instances. The model was trained for 500 epochs with a batch size of 512. The proposed algorithm has been released on GitHub: https://github.com/HIGISX/EMCLP-DRL (accessed on 16 July 2026).

Three evaluation metrics were adopted to assess the performance of different models. The average objective value (Avg-Obj) denotes the average EMCLP objective value obtained on the test instances, reflecting the weighted covered demand under the service radius constraint. A larger Avg-Obj indicates better solution quality. The reported Time metric represents the runtime associated with solution generation, measured in seconds. For Gurobi and the heuristic or metaheuristic baseline methods, Time denotes the runtime required to obtain the final solution in a single optimization or search run. For the DRL method, Time denotes the online inference time after offline training. The optimality gap (Gap) measures the relative difference between each method and the Gurobi reference solution, calculated as Gap = $(Obj_{Gurobi} - Obj_{method})/Obj_{Gurobi} \times 100\%$. A smaller Gap indicates that the obtained solution is closer to the reference optimum.

The proposed DRL method was compared with both an exact solver and several commonly used heuristic and metaheuristic algorithms. Gurobi was selected as the reference exact solver because it can provide optimal or high-quality reference solutions for NP-hard mixed-integer optimization problems. To ensure a fair comparison, no time limit was imposed on Gurobi, and the remaining parameters were kept at their default settings. In addition, GA, SA, PSO, and NSGA-II were selected as representative heuristic and evolutionary baselines. All methods were tested on the same workstation. Gurobi and the

heuristic algorithms were mainly executed on the CPU, whereas the training and inference processes of the DRL model were conducted on the GPU.

For the heuristic and metaheuristic algorithms, the search budgets were kept as consistent as possible. For GA, the population size was set to 100, the maximum number of iterations was set to 200, the crossover probability was set to 0.8, and the mutation probability was set to 0.2. For PSO and NSGA-II, the population size was set to 100 and the maximum number of iterations was set to 200. For SA, the maximum number of outer iterations was set to 200, and the Markov chain length at each temperature was set to 100, making its search scale comparable to that of GA. The initial temperature, final temperature, and cooling coefficient of SA were set to 100, 10^{-3}, and 0.94, respectively. PSO adopted a linearly decreasing inertia weight from 0.9 to 0.4, with learning factors c1 = c2 = 2.0. For NSGA-II, the crossover and mutation probabilities were set to 0.4 and 0.2, respectively, with distribution indices ηc = 20 and ηm = 20. Since the proposed EMCLP is formulated as a weighted single-objective model, the nondominated solutions generated by NSGA-II were further ranked according to the unified EMCLP objective value, and the solution with the highest objective value was selected for comparison.

4.2.3. Experimental Results

To achieve a fair allocation of elderly care resources under the complex spatiotemporal constraints of Chaoyang District, Beijing, a deep reinforcement learning (DRL) approach was introduced, formulating the facility location problem as a sequential decision-making process. The encoder was employed to extract heterogeneous spatial demand features, while the decoder intelligently identified optimal layout solutions from the set of candidate locations. Under a service radius constraint of 2000 m, the model ultimately selected 30 optimal sites for new elderly care facilities, as illustrated in Figure 8. Diamonds indicate the optimal elderly care facility locations selected by the DRL model.

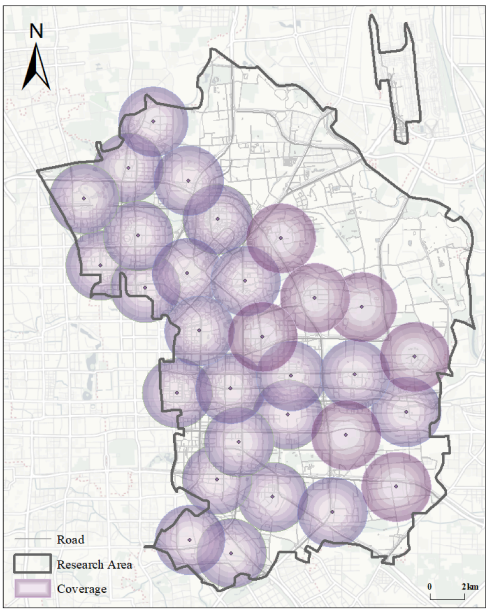


Figure 8. Optimal locations of elderly care facilities identified by the DRL.

Compared with exact optimization methods, the trained DRL model can rapidly generate high-quality solutions without repeated iterative searches. This characteristic becomes particularly valuable when the number of candidate sites increases, additional planning constraints are introduced, or multiple planning scenarios and sensitivity analyses need to be evaluated. Therefore, the computational efficiency results should be interpreted

as evidence of the scalability and adaptability of the proposed framework rather than as a direct policy advantage derived solely from shorter computation times.

To further evaluate the solution quality and computational efficiency of the proposed DRL approach, comparative experiments were conducted under three facility-number settings, namely M = 25, M = 30, and M = 35. The results are reported in Table 3.

Table 3. Comparison of different experimental methods.

	D = 5151, N = 1500, M = 25			D = 5151, N = 1500, M = 30			D = 5151, N = 1500, M = 35		
Methods	**Avg-Obj**	**Time**	**Gap**	**Avg-Obj**	**Time**	**Gap**	**Avg-Obj**	**Time**	**Gap**
Gurobi	11,259.39	24.87	0.00%	15,707.24	31.26	0.00%	15,995.74	39.58	0.00%
PSO	10,475.74	28.64	6.96%	14,642.43	35.17	6.78%	14,875.89	44.23	7.00%
GA	10,738.11	55.92	4.63%	14,931.57	68.46	4.94%	15,192.75	82.71	5.02%
SA	9472.87	3.26	15.87%	13,221.39	4.18	15.82%	13,784.16	5.03	13.83%
NSGA-II	10,864.19	128.35	3.51%	15,094.66	156.72	3.90%	15,365.51	181.46	3.94%
DRL	11,102.87	0.10	1.39%	15,445.71	0.12	1.66%	15,718.21	0.13	1.73%

Note: For DRL, Time denotes the online inference time after offline training. For Gurobi and the heuristic or metaheuristic baselines, Time denotes the runtime required to obtain the final solution in a single optimization or search run. Except for Gurobi, the reported Obj, Time, and Gap values are averaged over 1000 independent runs. Gap is calculated relative to the Gurobi objective value under the same setting.

As shown in Table 3, Gurobi achieved the highest objective values under all three settings and was therefore used as the reference optimum. However, its computational time increased from 24.87 s to 39.58 s as M increased from 25 to 35. In comparison, the proposed DRL method achieved objective values close to those of Gurobi, with gaps of only 1.39%, 1.66%, and 1.73% under M = 25, M = 30, and M = 35, respectively. Meanwhile, after offline training, the DRL model generated solutions within 0.10–0.13 s during online inference. By comparison, the reported times for Gurobi and the heuristic or metaheuristic baselines correspond to the runtime required to obtain final solutions in single optimization or search runs. This result indicates the strong post-training solution-generation efficiency of the DRL model, particularly for repeated scenario evaluation.

Compared with PSO, GA, SA, and NSGA-II, DRL achieved a better balance between solution quality and computational efficiency. Although NSGA-II obtained relatively small gaps, its computational time was much longer, reaching 128.35 s, 156.72 s, and 181.46 s under the three settings. SA was computationally efficient but produced larger optimality gaps, indicating insufficient solution quality. PSO and GA showed moderate solution quality but required longer computation times than DRL.

4.2.4. Parameter Sensitivity Analysis of Objective-Function Weights

The preceding algorithm comparison was conducted under the baseline objective-function weight setting ($\theta_1, \theta_2, \theta_3$ = 0.7, 0.2, 0.1). To further examine whether the optimization results were overly dependent on this specific parameter configuration, a sensitivity analysis was performed on the three objective-function weights. In this experiment, the demand points, candidate locations, service radius, number of selected facilities, and model constraints were kept unchanged, and only θ_1, θ_2, and θ_3 were varied. The analysis was conducted under the representative setting D = 5151, N = 1500, and M = 30. The results are reported in Table 4. The resulting solutions were evaluated using coverage rate, average service distance, the average Gini-related penalty of active facilities, and the active-facility Jaccard similarity relative to the baseline solution. Here, active facilities refer to selected facilities that actually serve at least one demand point.

Table 4. Sensitivity analysis of objective-function weights under D = 5151, N = 1500, and M = 30.

Setting	θ_1	θ_2	θ_3	Coverage Rate (%)	Avg. Service Distance (m)	Avg. Active (G)	Active-Facility Jaccard
W1	0.90	0.05	0.05	88.68	1207.6	0.2973	0.200
W2	0.80	0.10	0.10	88.13	1227.9	0.2973	0.935
W3	0.70	0.20	0.10	88.01	1226.7	0.2973	1.000
W4	0.60	0.30	0.10	86.47	1187.0	0.2910	0.250
W5	0.60	0.20	0.20	86.79	1191.0	0.2940	0.250
W8	0.40	0.40	0.20	85.54	1168.3	0.2910	0.224
W10	0.40	0.20	0.40	83.75	1146.8	0.2940	0.333
W12	0.30	0.20	0.50	79.02	1085.5	0.2910	0.333

Note: θ_1, θ_2, and θ_3 denote the weights of demand coverage, Gini-related inequality penalty, and travel-distance penalty, respectively. The active-facility Jaccard similarity is calculated relative to the baseline setting W3. Avg. active (G) is calculated based on facilities that actually serve at least one demand point; a lower value indicates a lower inequality penalty.

The results reveal a clear trade-off among demand coverage, inequality penalty, and service distance. Higher demand-coverage weights lead to better coverage performance: W1 and W2 achieve coverage rates of 88.68% and 88.13%, respectively, close to the baseline value of 88.01%. In contrast, increasing the distance-penalty weight reduces the average service distance from 1226.7 m (baseline) to 1085.5 m (W12), but coverage declines from 88.01% to 79.02%. This indicates that shorter travel distances are achieved at the expense of serving fewer elderly residents.

The G-related indicators show a similar pattern. As the inequality-penalty weight increases, active facilities tend to exhibit lower G-related penalty values. Although the change is modest, with the average active G decreasing from 0.2973 to about 0.2910, the results suggest that stronger equity preferences encourage the selection of lower-inequality locations.

Regarding solution stability, the active-facility Jaccard similarity between W2 and the baseline reaches 0.935, indicating a highly consistent facility layout near the baseline setting. Under more extreme weight combinations, the similarity decreases as the model adjusts facility selections to reflect different planning priorities. Overall, the baseline configuration provides a balanced emphasis on demand coverage, inequality reduction, and distance efficiency, while the high similarity observed in neighboring settings suggests that the main conclusions remain robust across a reasonable range of planning preferences.

4.2.5. Optimization of Elderly Care Resource Allocation Based on the Max–Min Distance Algorithm

Based on the identification of 30 optimal candidate locations for elderly care facilities, this section further explores how to scientifically determine the functional attributes of each site. To achieve precise and differentiated supplementation, a weighted composite inequality index I_k is introduced. This index is designed to reflect the existing degree of imbalance across different facility types and to enable demand-oriented resource allocation through a targeted distribution mechanism.

Demand-Driven Allocation Strategy for Elderly Care Facility Quotas

First, a weighted composite inequality index model is constructed to quantify the combined effects of different travel modes on spatial equity:

$$I_k = \alpha \cdot G_{walk,k} + \beta \cdot G_{drive,k} \tag{26}$$

where k denotes the facility type; $G_{\text{walk},k}$ and $G_{\text{drive},k}$ represent the Gini coefficients under walking and driving modes, respectively; and α and β are the corresponding weighting coefficients. The model follows a compensatory logic in which the degree of existing inequity is positively correlated with the allocation of additional facilities, and is used to determine the number of new facilities for each facility type:

$$N_k = N_{total} \times \frac{I_k}{\sum I_k} \tag{27}$$

The results indicate that Social and Cultural (SC) facilities exhibit the most pronounced spatial inequality in the baseline assessment, with the highest Gini coefficient for walking accessibility ($\text{Gini}_{\text{walk}} = 0.837$); accordingly, they are assigned the highest priority in the optimization process. Medical institution facilities show the second-highest level of spatial inequality and are therefore given a medium allocation priority. In contrast, Daily Care facilities display a relatively balanced existing spatial distribution and are assigned the lowest priority. Based on this priority ranking, the optimized allocation results determine that 7 Daily Care facilities, 11 Medical institution facilities, and 12 Social and Cultural facilities are to be newly established.

Functional Attribute Allocation and Spatial Mapping Based on Max–Min Distance Algorithm

After determining the functional quotas using the weighted composite inequality index (I_k), the Max–Min Distance Algorithm was introduced to refine the assignment of functional attributes to the 30 newly selected elderly care facility sites, with the aim of maximizing overall service effectiveness through spatial configuration. The optimization results are shown in Figure 9. Diamonds indicate the optimal elderly care facility locations selected by the DRL model. The core logic of this algorithm lies in iteratively calculating the spatial impedance between each candidate site to be assigned and existing facilities of the same type, thereby ensuring that newly allocated resources achieve optimal spatial exclusivity and complementarity in their geographic distribution. As a result of this procedure, the 30 newly added facilities form a coordinated functional–spatial pattern across Chaoyang District, as illustrated in Figure 10.

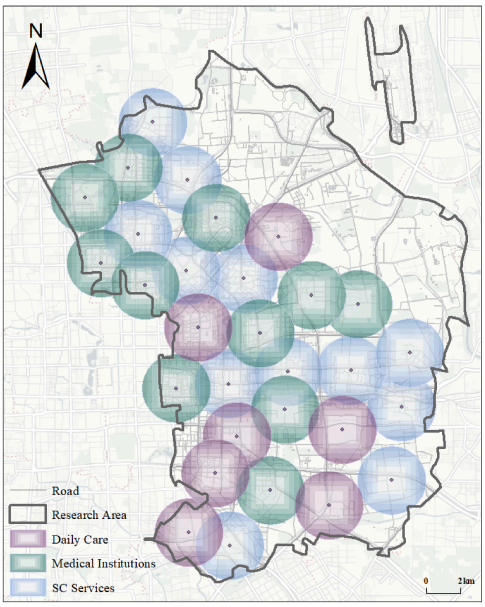


Figure 9. Spatial allocation and coverage layout map of various types of elderly care facilities.

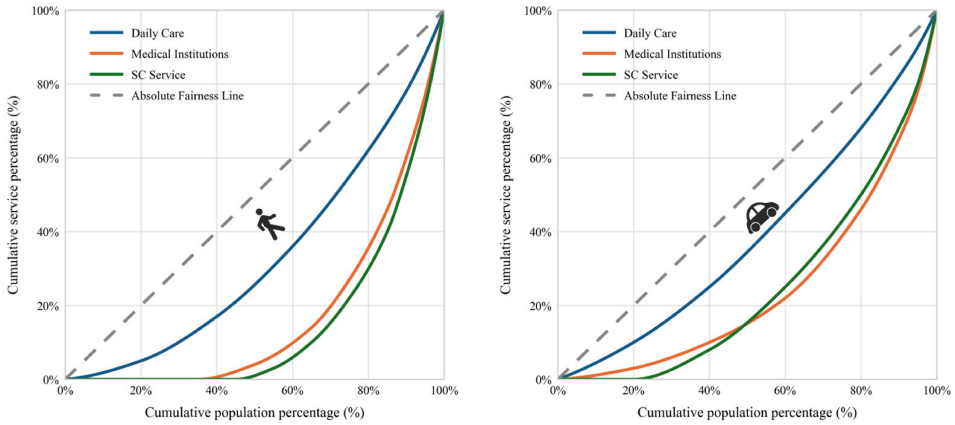


Figure 10. Lorenz curves after optimization under two travel scenarios: (**a**) Lorenz curves in walking state; (**b**) Lorenz curves under drive motion conditions.

The optimization results indicate that the finalized 30 elderly care facility locations exhibit clear characteristics of functional synergy and spatial complementarity at the district scale. In terms of facility-type distribution, different categories of elderly care facilities form a relatively well-defined functional division in space. Social and Cultural service facilities are predominantly allocated to areas with relatively weak existing social service provision, particularly in zones outside the urban core, where they serve a complementary role. This configuration helps alleviate social service accessibility imbalances caused by uneven historical facility distribution, thereby supplementing the existing elderly care service system and mitigating local service coverage deficiencies resulting from facility over-concentration. Medical service facilities are mainly distributed within the transitional belt between the urban core and peripheral areas, enhancing medical accessibility and emergency response capacity at key spatial nodes. Daily Care facilities are primarily targeted toward areas with highly concentrated elderly populations, which helps relieve the supply–demand pressure on existing elderly care resources in the urban core.

Overall, guided by the Max–Min Distance optimization mechanism, the resulting site-selection scheme forms a spatial layout characterized by deliberate spatial differentiation. On the one hand, it effectively avoids excessive proximity and inefficient competition among facilities of the same type at the geographic level; on the other hand, it promotes a hierarchical and coordinated configuration of the elderly care service system at the functional level. Consequently, the scheme significantly enhances the spatial equity of elderly care service provision while maintaining high service coverage efficiency.

4.2.6. Evaluation of Optimization Performance

To evaluate the effectiveness of the proposed EMCLP model in enhancing the spatial equity of elderly care service provision, the Lorenz curves and Gini coefficients of accessibility for the three categories of elderly care facilities were compared before and after optimization. The corresponding results are illustrated in Figure 10 and Table 5.

From the perspective of the Lorenz curve, the curves for all three categories of elderly care facilities shifted noticeably toward the Line of Equality after optimization, indicating a more balanced spatial distribution of elderly care accessibility. Prior to optimization, the Lorenz curves exhibited pronounced downward curvature, suggesting that a relatively small number of areas concentrated a disproportionately high share of elderly care resources, while the majority of the elderly population had comparatively limited access to services. Following optimization, the degree of curvature was substantially reduced, and the deviation between the cumulative population proportion and the cumulative

accessibility proportion decreased significantly. This result demonstrates that the spatial allocation of elderly care resources evolved from a relatively concentrated pattern toward a more equitable distribution.

Table 5. Comparison of Gini Coefficients for Multi-mode Facility Accessibility Before and After Optimization.

Facility Type	Mode	Before Optimization	After Optimization	Relative Improvement
Daily Care	Drive	0.345	0.250	27.54%
	Walk	0.459	0.350	23.75%
Medical Institutions	Drive	0.619	0.480	22.46%
	Walk	0.760	0.650	14.47%
SC Service	Drive	0.556	0.460	17.27%
	Walk	0.837	0.720	13.98%

First, among the three facility categories, Daily Care facilities exhibited the most substantial improvement in spatial equity. Under the driving scenario, the Gini coefficient decreased from 0.345 to 0.250, representing a relative improvement of 27.54%. Under the walking scenario, the Gini coefficient declined from 0.459 to 0.350, corresponding to a relative improvement of 23.75%. These results indicate that the optimized spatial distribution of Daily Care facilities achieved the highest level of equity, thereby better satisfying older adults' needs for convenient access to nearby care services. Second, the spatial equity of Medical Institutions and Spiritual, Cultural, and SC Service facilities also improved considerably following optimization. For Medical Institutions, the relative improvement rates reached 22.46% and 14.47% under the driving and walking scenarios, respectively. Similarly, SC Service facilities achieved relative improvements of 17.27% and 13.98% under the two travel modes. Although the post-optimization Gini coefficients of these facility types remained relatively high, the severe spatial inequality in accessibility was substantially mitigated by the optimization model. This improvement is particularly noteworthy given the inherently higher construction costs and larger service catchment areas associated with these facility types. Finally, a comparison across travel modes reveals that the Gini coefficients of all facility categories were consistently lower under the driving scenario than under the walking scenario, and the relative improvements achieved through optimization were generally greater. This pattern is also visually evident in Figure 10, where the Lorenz curves under the driving scenario (Figure 10b) are noticeably closer to the Line of Equality than those under the walking scenario (Figure 10a). These findings suggest that automobile-based travel can effectively overcome spatial distance constraints and physical environmental barriers, thereby further amplifying the positive impact of the optimization model on accessibility equity.

By jointly examining the results presented in Figure 10 and Table 5, the inherent trade-off between efficiency and equity can be further elucidated. Under the proposed optimization scheme, resources were preferentially allocated to underserved areas, which resulted in a slight reduction in the coverage efficiency of certain individual facilities. Nevertheless, the overall coverage rate remained at 98.3% of the benchmark optimal solution. At the same time, the Gini coefficients of all facility types decreased substantially, with a weighted average improvement of approximately 18.6%. These findings indicate that the proposed EMCLP framework achieves a significant enhancement in spatial equity at the cost of less than 2% efficiency loss. In other words, the model realizes a Pareto improvement between efficiency and equity, demonstrating its ability to effectively balance

the dual objectives of maximizing service coverage and promoting equitable access to elderly care services.

5. Discussion

The results of this study reveal significant spatial inequalities in the allocation of elderly care service resources within Chaoyang District, Beijing, with substantial differences in accessibility levels and equity performance across facility types. In particular, the Gini coefficients of SC Service and Medical Institutions were considerably higher than those of Daily Care facilities, indicating a pronounced spatial concentration of elderly care resources and suggesting that a large proportion of older adults are unable to access services on an equitable basis.

Beyond the methodological development, the empirical and optimization findings further contribute to recent discussions on equity-oriented elderly care facility planning. Recent studies have shown that elderly care facilities often suffer from spatial accessibility inequality and supply–demand mismatch, especially in large and high-density cities [52,53]. Consistent with these studies, this research confirms that accessibility inequality remains a key issue in elderly care service provision. More importantly, the results show that such inequality varies across facility types, with daily care facilities exhibiting relatively balanced accessibility patterns and medical and social-cultural facilities showing stronger spatial concentration [54,55]. This finding echoes recent evidence on the differentiated equity outcomes of hierarchical older adult care facilities and suggests that elderly care facilities should be evaluated and optimized according to their functional characteristics. In addition, the comparison between walking and driving scenarios supports recent transport-accessibility research showing that travel mode significantly affects both accessibility and equity outcomes [56,57]. The optimization results further extend recent multi-objective facility location studies by demonstrating that targeted allocation can improve population-weighted accessibility equity while maintaining high coverage efficiency. Therefore, the findings provide empirical support for differentiated, mobility-sensitive, and equity-oriented elderly care facility planning in high-density urban areas.

The optimization results proposed in this study not only identify suitable locations for newly developed Elderly Care facilities but also provide practical policy guidance for the allocation of Elderly Care service resources. First, in densely developed urban core areas, reliance on new facility construction alone is often constrained by limited land availability and high development costs. Therefore, priority should be given to enhancing elderly care service capacity through the renovation of existing facilities, capacity expansion, and the multifunctional reuse of existing spaces. Second, improving transportation accessibility represents another critical pathway for enhancing the equity of elderly care services. The results indicate that spatial disparities in Elderly Care facilities accessibility are substantially lower under the driving scenario than under the walking scenario. Consequently, strengthening public transportation networks, optimizing active transportation systems, and improving barrier-free infrastructure can effectively expand the service coverage of elderly care facilities and alleviate spatial inequalities in access.

Furthermore, Elderly Care facilities planning should be closely integrated with urban renewal initiatives and territorial spatial planning strategies. Elderly Care facilities should be incorporated into community public service facility standards, with higher provision requirements established for newly developed residential areas. At the same time, policymakers should encourage the adaptive reuse of underutilized public buildings, community service centers, and other existing spaces for elderly care purposes. Such measures can facilitate the targeted supplementation of elderly care resources and promote a more balanced and equitable spatial distribution of services.

Although equity-oriented elderly care facility allocation strategies can effectively alleviate spatial inequalities, their practical implementation remains subject to several challenges. First, the optimal locations identified for new facilities are often situated in underserved areas where land resources are scarce. As a result, local governments may face difficulties related to land acquisition, as well as increasing construction and development costs during the implementation process. Second, the provision of elderly care facilities involves multiple stages, including capital investment, operational management, and long-term maintenance. Under conditions of limited financial resources, it is difficult to simultaneously satisfy the service demands of all regions. Furthermore, elderly care facility planning inevitably requires a trade-off between service efficiency and spatial equity. From a theoretical perspective, prioritizing facility development in underserved areas can substantially reduce disparities in accessibility. However, such areas often have lower population densities and smaller potential service markets, which may negatively affect facility utilization efficiency. Therefore, future elderly care planning should seek an appropriate balance among coverage efficiency, spatial equity, and development costs according to the city's stage of development and fiscal capacity.

The sensitivity analysis further confirms that this trade-off is not caused by a single arbitrary weight configuration. Around the baseline setting, the model maintains similar coverage performance and a highly consistent active-facility layout, while stronger distance or inequality penalties lead to expected changes in the selected locations and service outcomes. This indicates that the proposed EMCLP framework can flexibly reflect different planning preferences while preserving an interpretable balance among demand coverage, inequality reduction, and travel-distance efficiency.

A further comparison of the optimization results across different facility types and travel modes reveals substantial differences in average accessibility, spatial equity, and the efficiency–equity trade-off. Daily Care facilities, characterized by relatively high initial coverage levels and a more balanced spatial distribution, achieved significant improvements in equity with limited resource investment, demonstrating a strong synergy between efficiency and equity. In contrast, Medical Institutions and SC Service were more strongly affected by the spatial concentration of resources. Although their levels of equity improved considerably after optimization, their Gini coefficients remained relatively high, indicating that further equity improvements would require greater resource inputs and investment costs. Across different travel modes, the driving scenario consistently exhibited higher average accessibility and lower Gini coefficients than the walking scenario, suggesting that improved transportation accessibility can simultaneously enhance service efficiency and spatial equity. By contrast, the walking scenario was more strongly constrained by distance-decay effects and the limited mobility of older adults, resulting in more pronounced inequalities in service access. Overall, Daily Care facilities are more conducive to achieving the simultaneous optimization of efficiency and equity, whereas Medical Institutions and SC Service face a more evident efficiency–equity trade-off. By explicitly incorporating equity into the optimization objective, the proposed EMCLP model effectively reduces spatial inequality while maintaining a high level of coverage efficiency, thereby providing a scientific basis for the precise and equitable allocation of elderly care service resources.

The EMCLP model proposed in this study provides a feasible technical pathway for achieving the coordinated optimization of efficiency and equity by explicitly incorporating equity considerations into the facility location decision-making process.

This study does not aim to identify the causal mechanisms or socioeconomic determinants of spatial inequality in elderly care service provision. Accordingly, spatial regression or spatial econometric models were not adopted as the main analytical tools. Instead,

the diagnosed accessibility and equity disparities were transformed into a constrained location-allocation optimization problem. Future research could integrate spatial econometric analysis to further examine the driving factors of inequity and incorporate such explanatory findings into adaptive optimization models.

6. Conclusions

This study contributes to equity-oriented elderly care facility planning by developing an optimization approach that integrates accessibility assessment, spatial equity evaluation, and facility location modeling. Methodologically, the Equity Maximum Covering Location Problem is formulated by embedding population-weighted accessibility inequality and travel impedance into the traditional maximal covering location problem. A deep reinforcement learning-based solution strategy is further developed by treating facility allocation as a sequential decision-making process. This allows the model to adaptively evaluate the marginal contribution of candidate sites in terms of coverage improvement, inequality reduction, and distance efficiency under complex spatial constraints. Beyond the methodological development, the optimization results also offer several planning implications. The results indicate that accessibility inequality in elderly care services varies across facility types: daily care facilities generally exhibit more balanced accessibility patterns, whereas medical and social-cultural facilities are more likely to show spatial concentration. The comparison between walking and driving scenarios further suggests that transportation accessibility plays an important role in shaping spatial equity outcomes. In addition, the optimization results show that efficiency and equity are not necessarily in conflict, as targeted facility allocation can improve accessibility equity while maintaining a high level of coverage efficiency. These findings provide empirical support for differentiated and equity-oriented elderly care facility planning in high-density urban areas.

The results suggest that spatial equity in elderly care services is inherently facility-type dependent rather than uniformly distributed across service categories. Facilities with localized and high-frequency service demands, such as Daily Care facilities, tend to exhibit relatively balanced accessibility patterns, whereas specialized facilities with larger service catchments, such as Medical Institutions and SC Service facilities, are more likely to develop spatial concentration effects. This finding indicates that the mechanisms generating accessibility inequality vary across facility functions and should therefore be addressed through differentiated planning strategies.

The comparison between walking and driving scenarios further reveals that transportation accessibility functions as an equity moderator. Improvements in mobility effectively reduce the spatial friction between service supply and population demand, thereby mitigating accessibility inequality. Therefore, spatial equity should be understood not only as a consequence of facility distribution but also as an outcome jointly shaped by transportation infrastructure and service location patterns.

The empirical results challenge the conventional assumption that efficiency and equity are necessarily conflicting objectives. The EMCLP results demonstrate that substantial improvements in accessibility equity can be achieved with only marginal reductions in coverage efficiency. This suggests the existence of a nonlinear efficiency–equity relationship, in which carefully targeted facility allocation can generate significant equity gains before substantial efficiency losses emerge.

This study focuses on the equity-oriented optimization of the spatial layout of elderly care facilities and develops an integrated methodological framework that combines spatial accessibility assessment, equity measurement, and resource allocation optimization. While ensuring a basic level of service coverage, spatial equity constraints are embedded into the maximal covering location model to achieve equity-oriented facility location optimization.

Empirically, the proposed EMCLP-based planning strategy improves equity outcomes while maintaining a high level of overall service coverage. The model allocates new facilities in a differentiated manner across functional types, consistent with observed inequity levels: facility types exhibiting larger Gini-based disparities receive more new sites (12 for social and cultural services and 11 for medical institutions), whereas daily care facilities with relatively balanced distributions receive fewer additions (7 sites). This targeted expansion helps reduce structural imbalances across the existing elderly care service system. After further refinement using the Max–Min Distance Algorithm, the resulting layout exhibits improved functional complementarity and a clearer hierarchical organization.

From a computational perspective, DRL provides a practical advantage for large-scale scenario evaluation after offline training. For the same EMCLP instance, the trained DRL model produced a high-quality feasible solution in 0.12 s during online inference, achieving 98.3% of the reference objective value obtained by Gurobi, which required 31.26 s to solve the corresponding single optimization instance. These results suggest that the trained DRL model can support rapid solution generation with near-optimal performance, making it particularly useful for repeated scenario simulations and sensitivity analyses in urban planning. Although the proposed approach achieves promising results in the empirical analysis, several limitations remain. This study focuses on using accessibility inequality as a measurable and operational proxy for spatial equity; however, this representation does not fully capture all dimensions of social equity. Given the substantial heterogeneity among older adults in terms of socioeconomic status, health conditions, disability levels, affordability of services, and vulnerability to environmental and climate-related risks, future research could incorporate indicators of population vulnerability, health status, income levels, long-term care needs, and environmental risk factors into the optimization framework. In doing so, a more comprehensive equity evaluation system could be established, thereby providing stronger support for more targeted decision-making in elderly care planning. "Additionally, the model lacks explicit consideration of facility capacity constraints, such as bed availability and service load limits, which could lead to service demand exceeding the carrying capacity of specific facilities. Furthermore, while the objective functions, parameter settings, and the deep reinforcement learning (DRL) algorithmic framework developed in this study are inherently generic and structurally designed for cross-city transferability, our current empirical experiment was limited to Chaoyang District, Beijing. This single-site focus is primarily due to the significant challenges in acquiring comprehensive, high-resolution multi-source spatial data (e.g., precise elderly population grids and 3D building footprints) across different urban environments. However, the proposed DRL framework possesses strong scalability and transferability. By simply replacing the input spatial datasets and retraining the agent, the model can be readily adapted to evaluate and optimize facility layouts in other cities with varying population structures, densities, and transportation systems. Future research will aim to overcome these data acquisition barriers to conduct cross-city comparative experiments, thereby further validating the framework's robustness and generalizability across diverse urban contexts.

Furthermore, the generalization performance of the deep reinforcement learning model inherently depends on the quality of training data and the choice of parameter configurations. From a computational perspective, the proposed DRL model requires an offline training stage before deployment. In our experiments, training under each scenario configuration typically required approximately 3–5 h on the specified workstation. This offline training cost should be acknowledged, particularly when the study area, candidate facility set, or planning constraints change substantially and model retraining becomes necessary. Nevertheless, once trained, the learned policy can be reused to generate solutions for multiple planning scenarios, with online inference requiring only 0.10–0.13 s in our

experiments. Therefore, the proposed approach shifts the main computational burden from repeated optimization to one-time offline training, supporting rapid scenario testing and multi-scheme comparison in practical planning applications. However, its applicability across diverse urban scales and spatial structures still requires further empirical validation. Overall, this study develops a novel optimization framework for elderly care facility location planning, shifting the objective from a sole focus on service coverage maximization to a comprehensive optimization that balances efficiency and spatial equity. An intelligent site selection framework based on deep reinforcement learning is proposed, demonstrating strong methodological scalability and substantial practical potential. The framework provides robust decision support for optimizing the spatial layout of elderly care facilities, improving community-level service networks, and guiding equity-oriented public resource allocation in the context of megacities.

Author Contributions: Conceptualization, Siyu Zhao and Shaohua Wang; methodology, Siyu Zhao; software, Hao Wang; validation, Siyu Zhao and Hao Wang; formal analysis, Siyu Zhao and Haojian Liang; investigation, Siyu Zhao and Hong Gao; resources, Siyu Zhao and Jingyi Zhou; data curation, Siyu Zhao and Hong Gao; writing—original draft preparation, Siyu Zhao; writing—review and editing, Haojian Liang and Jingyi Zhou; visualization, Siyu Zhao and Chang Liu; supervision, Shaohua Wang, Jingyi Zhou and Ning Zhang; project administration, Shaohua Wang; funding acquisition, Shaohua Wang. All authors have read and agreed to the published version of the manuscript.

Funding: This research was supported by a grant from the State Key Laboratory of Geographic Information Science and Technology, grant number 2024KFJJ009, and funded by China Southern Power Grid Company Limited, grant number ZBKJXM20240174; the National Key R&D Program of China, grant number 2023YFF0805904; the Talent Introduction Program Youth Project of the Chinese Academy of Sciences, grant numbers E43302020D, E2Z105010F; the National Natural Science Foundation of China, grant number 42471495; the Deployment Program of the Aerospace Information Research Institute, Chinese Academy of Sciences (AIRCAS), grant number E4Z202021F; and the Guangzhou Institute of Energy Conversion, Chinese Academy of Sciences, grant number E4C1020301.

Data Availability Statement: Data will be made available on request.

Acknowledgments: Thanks to all the reviewers and editors.

Conflicts of Interest: The authors declare no competing financial interest.

References

1. Fang, E.F.; Fang, Y.; Chen, G.; Wang, H.L.; Zhang, J.; Wu, C.; Liao, J.; Xie, C.; Liu, X.; Wang, K.; et al. Adapting health, economic and social policies to address population aging in China. *Nat. Aging* **2025**, *5*, 2176–2187. [CrossRef] [PubMed]
2. Jia, L.; Du, Y.; Chu, L.; Zhang, Z.; Li, F.; Lyu, D.; Zhu, M.; Jiao, H.; Song, Y.; Shi, Y.; et al. Prevalence, risk factors, and management of dementia and mild cognitive impairment in adults aged 60 years or older in China: A cross-sectional study. *Lancet Public Health* **2020**, *5*, e661–e671. [PubMed]
3. Bai, R.; Liu, Y.; Zhang, L.; Dong, W.; Bai, Z.; Zhou, M. Projections of future life expectancy in China up to 2035: A modelling study. *Lancet Public Health* **2023**, *8*, e915–e922. [CrossRef] [PubMed]
4. Cheng, T.; Liu, C.; Yang, H.; Wang, N.; Liu, Y. From service capacity to spatial equity: Exploring a multi-stage decision-making approach for optimizing elderly-care facility distribution in the city centre of Tianjin, China. *Sustain. Cities Soc.* **2022**, *85*, 104076. [CrossRef]
5. Mahmut, M.; Yin, P.; Peng, B.; Wu, J.; Wang, T.; Yuan, S.; Zhang, Y. Examining Spatial Accessibility and Equity of Public Hospitals for Older Adults in Songjiang District, Shanghai. *ISPRS Int. J. Geo-Inf.* **2024**, *13*, 403. [CrossRef]
6. Tao, Z.; Cheng, Y.; Dai, T.; Rosenberg, M.W. Spatial optimization of residential care facility locations in Beijing, China: Maximum equity in accessibility. *Int. J. Health Geogr.* **2014**, *13*, 33. [CrossRef] [PubMed]
7. Zhang, Y.; Zhu, J.; Li, F.; Wang, Y. Site selection of elderly care facilities based on multi-source spatial big data and integrated learning. *ISPRS Int. J. Geo-Inf.* **2024**, *13*, 451. [CrossRef]
8. Church, R.; ReVelle, C. The maximal covering location problem. In *Papers of the Regional Science Association*; Springer: Berlin/Heidelberg, Germany, 1974; Volume 32, pp. 101–118.

9. Hosseini, M.M.; Beheshti, S.; Heydari, J.; Zangiabadi, M.; Zargoush, M. Elderly care facility location in the face of the climate crisis: A case study in Canada. *Int. J. Disaster Risk Reduct.* **2024**, *108*, 104516. [CrossRef]
10. Li, W.; Zhai, G.; Chen, W. Location-allocation of fixed shelters for the elderly from the perspective of needs for refuge: A case of Hefei, China. *Int. J. Disaster Risk Reduct.* **2023**, *92*, 103717. [CrossRef]
11. Xing, L.; Chen, Q.; Liu, Y.; He, H. Evaluating the accessibility and equity of urban health resources based on multi-source big data in high-density city. *Sustain. Cities Soc.* **2024**, *100*, 105049. [CrossRef]
12. Gu, T.; Li, L.; Li, D. A two-stage spatial allocation model for elderly healthcare facilities in large-scale affordable housing communities: A case study in Nanjing City. *Int. J. Equity Health* **2018**, *17*, 183. [CrossRef] [PubMed]
13. Yao, Y.; Wang, Y.; Liang, L.; Yan, X.; Dong, A.; Guan, Q.; Luo, P. Evaluation and Spatial Optimization Model of Urban Medical Resource Distribution Considering Equity and Efficiency. *Trans. GIS* **2025**, *29*, e70089. [CrossRef]
14. Wan, D.; Liu, H.; Guo, J.; Guo, L.; Qi, D.; Zhang, S.; Li, P.; Fukuda, H. Spatial Distribution and Accessibility Measurements for Elderly Day Care Centers in China's Urban Built-up Area: The Case of Tianjin Nankai District. *Buildings* **2022**, *12*, 1413. [CrossRef]
15. Li, Z.; Diaoxia, H.; Jian, Z. Spatial Distribution and Factors Influencing Elderly Care Service Facilities based on Accessibility Evaluation—Taking Wuxi City as an Example. *J. Resour. Ecol.* **2024**, *15*, 130–139.
16. Zhou, X.; Cao, K. Spatial multi-objective optimization of institutional elderly-care facilities: A case study in Shanghai. *Int. J. Appl. Earth Obs. Geoinf.* **2023**, *122*, 103436. [CrossRef]
17. Shi, J.; Liu, X.; Feng, Z. Age-friendly cities and communities and cognitive health among Chinese older adults: Evidence from the China Health and Retirement Longitudinal Studies. *Cities* **2023**, *132*, 104072. [CrossRef]
18. Xiang, L.; Shen, G.Q.; Tan, Y.; Liu, X. Emerging evolution trends of studies on age-friendly cities and communities: A scientometric review. *Ageing Soc.* **2021**, *41*, 2814–2844.
19. Bonaccorsi, G.; Manzi, F.; Del Riccio, M.; Setola, N.; Naldi, E.; Milani, C.; Giorgetti, D.; Dellisanti, C.; Lorini, C. Impact of the built environment and the neighborhood in promoting the physical activity and the healthy aging in older people: An umbrella review. *Int. J. Environ. Res. Public Health* **2020**, *17*, 6127. [CrossRef] [PubMed]
20. De Keijzer, C.; Tonne, C.; Sabia, S.; Basagaña, X.; Valentín, A.; Singh-Manoux, A.; Antó, J.M.; Alonso, J.; Nieuwenhuijsen, M.J.; Sunyer, J.; et al. Green and blue spaces and physical functioning in older adults: Longitudinal analyses of the Whitehall II study. *Environ. Int.* **2019**, *122*, 346–356. [CrossRef] [PubMed]
21. Salami, A.; Afshar-Nadjafi, B.; Amiri, M. A two-stage optimization approach for healthcare facility location-allocation problems with service delivering based on genetic algorithm. *Int. J. Public Health* **2023**, *68*, 1605015. [CrossRef] [PubMed]
22. Liu, S.; Wang, Y.; Zhou, D.; Kang, Y. Two-step floating catchment area model-based evaluation of community care facilities' spatial accessibility in Xi'an, China. *Int. J. Environ. Res. Public Health* **2020**, *17*, 5086. [CrossRef] [PubMed]
23. Liu, L.; Lyu, H.; Zhao, Y.; Zhou, D. An improved two-step floating catchment area (2SFCA) method for measuring spatial accessibility to elderly care facilities in Xi'an, China. *Int. J. Environ. Res. Public Health* **2022**, *19*, 11465. [CrossRef] [PubMed]
24. Wang, M.; Qi, X.; Li, Z.; Li, J.; Dong, S. Evaluation of the suitability of elderly care in prefecture-level cities in China based on GIS. *Heliyon* **2023**, *9*, e16539. [CrossRef] [PubMed]
25. Rahman, S.U.; Smith, D.K. Use of location-allocation models in health service development planning in developing nations. *Eur. J. Oper. Res.* **2000**, *123*, 437–452. [CrossRef]
26. Mestre, A.M.; Oliveira, M.D.; Barbosa-Póvoa, A. Organizing hospitals into networks: A hierarchical and multiservice model to define location, supply and referrals in planned hospital systems. *OR Spectr.* **2012**, *34*, 319–348.
27. Talen, E.; Anselin, L. Assessing spatial equity: An evaluation of measures of accessibility to public playgrounds. *Environ. Plan. A* **1998**, *30*, 595–613. [CrossRef]
28. Tsou, K.W.; Hung, Y.T.; Chang, Y.L. An accessibility-based integrated measure of relative spatial equity in urban public facilities. *Cities* **2005**, *22*, 424–435. [CrossRef]
29. Drezner, Z.; Hamacher, H.W. (Eds.) *Facility Location: Applications and Theory*; Springer Science & Business Media: Berlin/Heidelberg, Germany, 2004.
30. Tao, Z.L.; Dai, T.Q.; Song, C.Q. Improving spatial equity-oriented location-allocation models of urban medical facilities. *Acta Geogr. Sin.* **2023**, *78*, 474–489.
31. Saldanha-da-Gama, F.; Wang, S. Distributionally Robust Facility Location. In *Facility Location Under Uncertainty: Models, Algorithms and Applications*; Springer International Publishing: Cham, Switzerland, 2024; pp. 203–226.
32. Digehsara, A.A.; Ji, M.; Ardestani-Jaafari, A.; Bidkhori, H. Equity-driven facility location: A two-stage robust optimization approach. *Comput. Oper. Res.* **2025**, *176*, 106920. [CrossRef]
33. Basu, S.; Sharma, M.; Ghosh, P.S. Metaheuristic applications on discrete facility location problems: A survey. *Opsearch* **2015**, *52*, 530–561. [CrossRef]
34. Guner, A.R.; Sevkli, M. A discrete particle swarm optimization algorithm for uncapacitated facility location problem. *J. Artif. Evol. Appl.* **2008**, *2008*, 861512. [CrossRef]

35. Liang, H.; Wang, S.; Li, H.; Zhou, L.; Chen, H.; Zhang, X.; Chen, X. Sponet: Solve spatial optimization problem using deep reinforcement learning for urban spatial decision analysis. *Int. J. Digit. Earth* **2024**, *17*, 2299211. [CrossRef]
36. Li, K.; Zhang, T.; Wang, R. Deep reinforcement learning for multiobjective optimization. *IEEE Trans. Cybern.* **2020**, *51*, 3103–3114. [CrossRef] [PubMed]
37. Zhong, E. Deep mapping—A critical engagement of cartography with neuroscience. *Geomat. Inf. Sci. Wuhan Univ.* **2022**, *47*, 1988–2002.
38. Liang, X.; Zhou, L.; Wang, S.; Zhao, X.; Xue, J.; Ding, Q.; Pan, Y. Spatiotemporal crime prediction and fairness-constrained spatial optimization with deep reinforcement learning for patrol region design. *Int. J. Appl. Earth Obs. Geoinf.* **2025**, *145*, 104973. [CrossRef]
39. Pinheiro, C.D.P.; Feliu, J.G.; Bertoncini, B.V. Addressing spatial heterogeneity and MAUP in urban transport geography: A multi-scale analysis of accessibility and warehouse location. *J. Transp. Geogr.* **2025**, *123*, 104078. [CrossRef]
40. Bolton, G.E.; Ockenfels, A. ERC: A theory of equity, reciprocity, and competition. *Am. Econ. Rev.* **2000**, *91*, 166–193. [CrossRef]
41. Zhao, P.; Li, S.; Liu, D. Unequable spatial accessibility to hospitals in developing megacities: New evidence from Beijing. *Health Place* **2020**, *65*, 102406. [CrossRef] [PubMed]
42. Zhang, W.; Cao, K.; Liu, S.; Huang, B. A multi-objective optimization approach for health-care facility location-allocation problems in highly developed cities such as Hong Kong. *Comput. Environ. Urban Syst.* **2016**, *59*, 220–230. [CrossRef]
43. Tu, W.J.; Zeng, X.; Liu, Q. Aging tsunami coming: The main finding from China's seventh national population census. *Aging Clin. Exp. Res.* **2022**, *34*, 1159–1163. [CrossRef] [PubMed]
44. Ju, Y.; Liang, Y.; Kong, J.; Wang, X.; Wen, S.; Shang, H.; Wang, X. 100-m resolution Age-Stratified Population Estimation from the 2020 China Census by Township (ASPECT). *Sci. Data* **2025**, *12*, 1058. [CrossRef] [PubMed]
45. Che, Y.; Li, X.; Liu, X.; Wang, Y.; Liao, W.; Zheng, X.; Zhang, X.; Xu, X.; Shi, Q.; Zhu, J.; et al. 3D-GloBFP: The first global three-dimensional building footprint dataset. *Earth Syst. Sci. Data* **2024**, *16*, 5357–5374. [CrossRef]
46. Guagliardo, M.F. Spatial accessibility of primary care: Concepts, methods and challenges. *Int. J. Health Geogr.* **2004**, *3*, 3. [CrossRef] [PubMed]
47. Lorenz, M.O. Methods of measuring the concentration of wealth. *Publ. Am. Stat. Assoc.* **1905**, *9*, 209–219. [CrossRef]
48. Kakwani, N.; Son, H.H. *Economic Inequality and Poverty: Facts, Methods, and Policies*; Oxford University Press: Oxford, UK, 2022.
49. Ceriani, L.; Verme, P. The origins of the Gini index: Extracts from Variabilità e Mutabilità (1912) by Corrado Gini. *J. Econ. Inequal.* **2012**, *10*, 421–443. [CrossRef]
50. Whitehead, J.L.; Pearson, A.; Lawrenson, R.; Atatoa-Carr, P. How can the spatial equity of health services be defined and measured? A systematic review of spatial equity definitions and methods. *J. Health Serv. Res. Policy* **2019**, *24*, 270–278. [CrossRef] [PubMed]
51. Cromley, G.A. Measuring differential access to facilities between population groups using spatial Lorenz curves and related indices. *Trans. GIS* **2019**, *23*, 1332–1351. [CrossRef]
52. Wang, S.; Zhou, J.; Liang, H.; Zhou, L.; Wang, Z.; Zhao, S.; Wang, H. Optimization of urban service facility allocation for the SDGs: Current status, innovations, and prospects. *Sustain. Cities Soc.* **2026**, *142*, 107291. [CrossRef]
53. Sun, X.; Cheng, Y.; Tao, Z. Spatial accessibility and equity of residential care facilities in Beijing from 2010 to 2020. *Health Place* **2024**, *86*, 103219. [CrossRef] [PubMed]
54. Wang, C.; Geng, X. Assessing the spatial equity of the aged care institutions based on the improved potential model: A case study in Shanghai, China. *Front. Public Health* **2024**, *12*, 1428424. [CrossRef] [PubMed]
55. Li, M.; Peng, P.; Zhu, H.; Ao, Y.; Zhou, Z. Exploring the equitable spatial planning on the accessibility of institutional elderly care in megacity: A study based on Chengdu, China. *Sustain. Cities Soc.* **2024**, *117*, 105998. [CrossRef]
56. Gu, M.; Li, S.; Zheng, G. Optimizing spatial accessibility and equity of hierarchical older adult care facilities using a multi-modal two-step floating catchment area method: A case study of Lin'an District, Hangzhou. *Front. Public Health* **2025**, *13*, 1559463. [CrossRef] [PubMed]
57. Ni, J.; Wang, Z.; Li, H.; Chen, J.; Long, Q. Spatial accessibility and equity of community healthcare: Unraveling the impact of varying time and transport mode. *Front. Public Health* **2024**, *12*, 1380884. [CrossRef] [PubMed]

Disclaimer/Publisher's Note: The statements, opinions and data contained in all publications are solely those of the individual author(s) and contributor(s) and not of MDPI and/or the editor(s). MDPI and/or the editor(s) disclaim responsibility for any injury to people or property resulting from any ideas, methods, instructions or products referred to in the content.